(12) INTERNATIONAL APPLICATION PUBLISHED UNDER THE PATENT COOPERATION TREATY (PCT)

(19) World Intellectual Property Organization
International Bureau

(43) International Publication Date
30 December 2015 (30.12.2015)

WIPO | PCT

(10) International Publication Number
WO 2015/200756 A1

(51) International Patent Classification:
C12Q 1/68 (2006.01) *G01N 33/00* (2006.01)

(21) International Application Number:
PCT/US2015/037894

(22) International Filing Date:
26 June 2015 (26.06.2015)

(25) Filing Language: English

(26) Publication Language: English

(30) Priority Data:
62/017,327 26 June 2014 (26.06.2014) US
62/017,332 26 June 2014 (26.06.2014) US

(71) Applicant: **PRESIDENT AND FELLOWS OF HARVARD COLLEGE** [US/US]; 17 Quincy Street, Cambridge, ME 02138 (US).

(72) Inventors: **GOLOVCHENKO, Jane, Andrew**; One Nowers Road, Lexington, MA 02420 (US). **LEVINE, Edlyn, Victoria**; 385 Huron Avenue, Apt. 2, Cambridge, MA 02138 (US). **NAGASHIMA, Gaku**; 2-5-34 Nishitsuda-cho, Matsue, Shimane, 690-0017 (JP). **BURNS, Michael Martin**; 70 Lansdowne Road, Arlington, Massachusetts 02472 (US).

(74) Agent: **LOBER, Theresa, A.**; T. A. Lober Patent Services, 60 Thoreau Street, Suite 215, Concord, MA 01742 (US).

(81) Designated States *(unless otherwise indicated, for every kind of national protection available)*: AE, AG, AL, AM, AO, AT, AU, AZ, BA, BB, BG, BH, BN, BR, BW, BY, BZ, CA, CH, CL, CN, CO, CR, CU, CZ, DE, DK, DM, DO, DZ, EC, EE, EG, ES, FI, GB, GD, GE, GH, GM, GT, HN, HR, HU, ID, IL, IN, IR, IS, JP, KE, KG, KN, KP, KR, KZ, LA, LC, LK, LR, LS, LU, LY, MA, MD, ME, MG, MK, MN, MW, MX, MY, MZ, NA, NG, NI, NO, NZ, OM, PA, PE, PG, PH, PL, PT, QA, RO, RS, RU, RW, SA, SC, SD, SE, SG, SK, SL, SM, ST, SV, SY, TH, TJ, TM, TN, TR, TT, TZ, UA, UG, US, UZ, VC, VN, ZA, ZM, ZW.

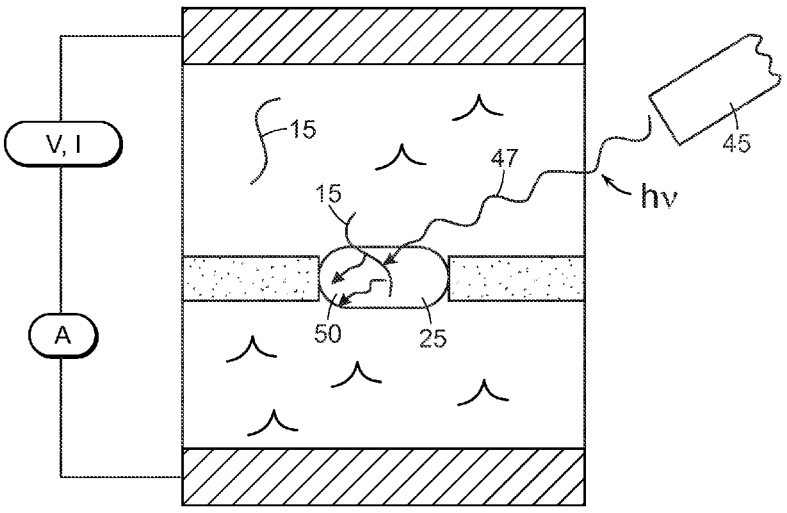
(84) Designated States *(unless otherwise indicated, for every kind of regional protection available)*: ARIPO (BW, GH, GM, KE, LR, LS, MW, MZ, NA, RW, SD, SL, ST, SZ, TZ, UG, ZM, ZW), Eurasian (AM, AZ, BY, KG, KZ, RU, TJ, TM), European (AL, AT, BE, BG, CH, CY, CZ, DE, DK, EE, ES, FI, FR, GB, GR, HR, HU, IE, IS, IT, LT, LU, LV, MC, MK, MT, NL, NO, PL, PT, RO, RS, SE, SI, SK, SM, TR), OAPI (BF, BJ, CF, CG, CI, CM, GA, GN, GQ, GW, KM, ML, MR, NE, SN, TD, TG).

Published:

— *with international search report (Art. 21(3))*

(54) Title: PORE-BASED BUBBLE CHAMBER

FIG. 8



(57) Abstract: There is herein provided a method for detecting an object, in which an object is translocated through a pore in a support structure from a first fluidic chamber containing an electrolytic solution including objects to be translocated through the pore to a second fluidic chamber containing the electrolytic solution for receiving an object that has translocated through the pore. The electrolytic solution in the pore is heated to a temperature that is at least a superheating temperature of the electrolytic solution and that is less than a temperature for homogeneous bubble nucleation in the electrolytic solution in the pore. A bubble in the pore is detected to indicate the presence of an object in the pore.

WO 2015/200756 A1

PORE-BASED BUBBLE CHAMBER

CROSS-REFERENCE TO RELATED APPLICATIONS

[0001] This application claims the benefit of U.S. Provisional Application No. 62/017,332, filed June 26, 2014, the entirety of which is hereby incorporated by reference. This application also claims the benefit of U.S. Provisional Application No. 62/017,327, filed June 26, 2014, the entirety of which is hereby incorporated by reference.

STATEMENT REGARDING FEDERALLY SPONSORED RESEARCH

[0001] This invention was made with Government support under Contract No. HG003703, awarded by the National Institutes of Health. The Government has certain rights in the invention.

BACKGROUND

[0002] This invention relates generally to the use of an aperture, such as a pore or nanopore, for sensing and detection of objects and species, such as molecules, and more particularly relates to the use of controlled vapor bubble formation at a pore for species sensing and detection, as well as for controlled experimental chamber conditions, at a pore.

[0003] There has been developed a wide array of device structures and techniques for detection and sensing of species as such molecules translocating through an aperture, and particularly though a nanoscale-sized pore, termed a nanopore. In general, such techniques are based on sensing the species itself directly as the species translocates through a pore, e.g., by electrical sensing. Various challenges in such direct-species electrical-sensing approaches remain, and have limited the ability to successfully achieve pore-based sensing. Pore-based experimentation has likewise been limited by the restrictions of conventional pore-based configurations.

SUMMARY

[0004] There is herein provided a method for detecting an object, in which an object is translocated through a pore in a support structure from a

first fluidic chamber containing an electrolytic solution including objects to be translocated through the pore to a second fluidic chamber containing the electrolytic solution for receiving an object that has translocated through the pore. The electrolytic solution in the pore is heated to a temperature that is at least a superheating temperature of the electrolytic solution and that is less than a temperature for homogeneous bubble nucleation in the electrolytic solution in the pore. A bubble in the pore is detected to indicate the presence of an object in the pore.

[0005] With this methodology, there is enabled the controllable initiation of homogeneous bubbles at the pore and detection of bubbles at a pore that operates as a bubble chamber to achieve highly reproducible homogeneous bubble nucleation and bubble detection. A wide range of electrical, chemical, optical, fluidic, and acoustic phenomena can be excited and observed in the high electric field and extreme environment of a pore with this platform. The apparatus and methodology herein enable a wide range of applications for indirectly detecting and identifying objects at or in a pore by detecting bubbles formed at the pore by such objects. The methodology further provides the ability to study reactions and optical and chemical phenomena in the fluidic environment of the pore. The objects can be biological molecules, polymer molecules, DNA, RNA, DNA and RNA fragments, single DNA bases, and other molecules and species.

[0006] Other features and advantages of the methodology will be apparent from the following description and accompanying drawings, and from the claims.

BRIEF DESCRIPTION OF THE DRAWINGS

[0007] Figure 1 is a schematic view of a pore-based object detection system;

[0008] Figure 2A is a cross-sectional view of the pore in Figure 1 with a focused path of ionic current through the pore shown for heating the pore;

[0009] Figure 2B is a cross-sectional view of the pore in Figure 1 with a bubble homogeneously nucleating at the pore center;

[0010] Figure 3 is a schematic cross sectional view of a pore geometry and boundary conditions for modeling Joule heating of the pore;

[0011] Figure 4 is a plot of temperature internal to a pore as a function of applied voltage across a pore for a 3 M KCl electrolyte and for five different pore geometries;

[0012] Figure 5 is a plot of temperature computed internal to a pore for a voltage pulse of 8.22 V applied for 10.4 microseconds across a 53.5 nm-radius, 71 nm-long pore with 3 M KCl electrolyte;

[0013] Figure 6 is a plot of vapor bubble nucleation rate as a function of distance from pore center, based on the thermal data from Figure 5

[0014] Figure 7 is a plot of ionic current flow through the pore in Figure 1 as a function of time, indicating the current blockage due to presence of a bubble at the pore;

[0015] Figure 8 is a schematic representation of the pore-based system of Figure 1 further including a laser beam source for energetically exciting an object located at the pore;

[0016] Figure 9 is a schematic cross-sectional view of a pore including an object which caused homogeneous nucleation of a bubble in the pore;

[0017] Figure 10 is a schematic representation of the pore in Figure 1 with an optical source directed to the pore for detecting reflection of light off of a vapor bubble at the pore;

[0018] Figure 11 is a schematic representation of the pore in Figure 1 with an acoustic wave detector positioned for detecting sound waves formed by vapor bubble production;

[0019] Figure 12 is a schematic view of an experimental pore-based object detection system including vapor bubble formation and detection capability;

[0020] Figures 13A and 13B are plots of measured ionic conductance of the pore in Figure 12 as a function of time as voltages of 8.22 V, 7.0 V, 6.09 V, 5.0 V, and 4.0 V are applied across the pore, and again as a voltage of 8.22 V is applied across the pore, respectively;

[0021] Figure 14A is a schematic view of an experimental pore-based object detection system built to enable laser beam direction and sensing through the pore;

[0022] Figures 14B and 14C are plots of measured pore conductance and photodiode current as a function of time for the experimental pore of Figure 9A, taken at the center of the pore and at the periphery of the pore, respectively; and

[0023] Figure 14D is a plot of t_p-t_i, from Figures 14B-14C, as a function of laser position.

DETAILED DESCRIPTION

[0024] Referring to Figure 1, there is provided a pore-based bubble chamber ystem 10 including a support structure 12, such as a solid state membrane, that separates two fluidic chambers 14, 16 in a closed fluidic system. At least one of the chambers, or both of the chambers, can include objects 15, such as a selected species, like molecules, to be sensed, detected, and/or analyzed. One chamber can be conventionally termed the *cis* chamber. The second chamber 16 can be termed the *trans* chamber. The membrane 12 includes an aperture 18, such as a pore, nanopore, hole, or other aperture, that is the sole path of fluidic communication and electrical conduction between the two fluidic chambers 14, 16.

[0025] The two chambers are provided with an ionically-conducting fluid, such as an electrolytic liquid. The presence and flow of the ionically-

conducting liquid through the pore 18 between the chambers can therefore be detected by sensing ionic current flow through the pore. Such ionic current flow is enabled by the connection of the two fluidic chambers in a closed-loop electrical circuit. Accordingly, each chamber 14, 16, is in electrical connection with an electrically conducting electrode 20, 22, whereby the liquid in each chamber is in electrical connection with an electrode. The electrodes are in turn connected in a circuit 24 that can include a controllable voltage source 26 or alternatively a current source. Application of a voltage between the electrodes 20, 22, produces an electric field across the pore in the support structure and a corresponding electrical potential between the two fluidic chambers, across the pore. The electric field drives ionic current through the pore, from one of the chambers to the other of the chambers, depending on the polarity of the applied voltage. The applied voltage also produces an electrophoretic force that drives through the pore any electrically charged species that are present in the liquid, such as electrically-charged molecules. The level of ionic current flow through the pore can be determined by the measuring the electrical current in the circuit 24 employing, e.g., electronic amplifiers and computer control, and other circuit elements for detecting conductance and current flow.

[0026] In one embodiment provided herein, the flow of ionic current through the pore is controlled to cause heating of the liquid at the site of the pore, through the cross section of the pore and along the pore length. In one method, this heating is produced by Joule heating. Joule heating is a process in which the ionic current flowing through the resistive constriction of the pore heats the liquid in the pore by release of energy, or dissipation of power, at the pore. The ionic solution gains this energy by moving through the electric field produced by the applied voltage across the pore. Referring to Figure 2A, the pore 18 is a fluidic constriction through which the ionic current 23 is focused. As the focused ionic current flows through the pore 18, a very localized heating by release of energy occurs at the pore region between the two chambers, in

the pore of the support structure. The pore thereby operates as a highly confined heating region between the two fluidic chambers.

[0027] The ions in the electrolytic solution gain energy by moving through the electric field produced by the applied voltage across the pore. Thus, by control of the voltage that is applied across the pore, the ionic current flow and corresponding Joule heating of the pore is controlled. This Joule heating can be controlled particularly to cause the liquid in the pore to be heated to a selected high temperature. In one embodiment, Joule heating is controlled to cause superheating in the pore. The term 'superheating' herein refers to a condition in which the electrolytic liquid in the pore is at a temperature that is above the equilibrium boiling point temperature of the liquid but is not boiling. This condition is achieved herein at atmospheric pressure. A superheating condition in the pore is a highly localized, excited metastable thermal state.

[0028] In considering the temperature of the pore that is produced by an applied voltage, and the voltage required to obtain superheating in the pore, it is first noted that as the voltage applied across the pore is increased, Joule heating of the electrolytic solution within the pore is correspondingly increased. The total power that is input to the system by Joule heating is proportional to the square of the applied voltage, i.e., V^2, and can be related to the thermal energy increase in the system over time, proportional to the change in temperature, T. Thus, as a very general rule, the temperature of the electrolytic solution in the pore is approximately proportional to the square of the applied voltage, i.e., V^2. But the exact dependence of electrolytic solution temperature on applied voltage is complicated due to the nonlinearity of the material properties of the system.

[0029] To determine the dependence of electrolytic solution temperature on applied voltage for a given pore system, for achieving superheating in the pore, it can be preferred to model the system with the nonlinear, inhomogeneous heat equation, using Joule heating as the heat source term,

and then solving the heat equation for the given pore geometry. This can be conducted, e.g., using an appropriate modeling tool, such as COMSOL MultiPhysics program from COMSOL, Inc., Burlington, MA. In such a modeling exercise, the heat equation is coupled with conditions of charge continuity and with Ohm's law to determine the source term. This can be accomplished, e.g., using the Joule Heating (jh) and Electric Currents (ec) modules in COMSOL. The equations take the form:

$$\nabla \cdot \boldsymbol{J} = \nabla \cdot (\sigma \boldsymbol{E}) = 0$$

$$\boldsymbol{J} = \sigma \boldsymbol{E} \qquad (1)$$

$$\boldsymbol{E} = -\nabla V$$

$$\rho C_p \frac{\partial T}{\partial t} = \nabla \cdot (\kappa \nabla T) + \boldsymbol{J} \cdot \boldsymbol{E},$$

where T is the temperature, V is the electrical potential, $\boldsymbol{E}$ is the electric field, and $\boldsymbol{J}$ is the current density. The support structure in which the pore is disposed is assumed to be non-conducting and the applied voltage is specified on the boundary far from the pore. The temperature condition can imposed on the boundary as $T = T_0$, where T_0 is the ambient temperature measured at the start of the Joule heating. This initial condition can be set as $T = T_0$ everywhere in the system. The density, ρ, heat capacity at constant pressure, C_p, thermal conductivity, κ, and electrical conductivity, σ, are all temperature-dependent properties of the electrolytic solution. Where material data for a selected aqueous electrolytic solution to be superheated in the pore system, which is at atmospheric pressure, is not available, there can be employed suitable values for the density, heat capacity and thermal conductivity, e.g., the values provided by IAPWS-95 (International Association for the Properties of Water and Steam formulation 1995 for the thermodynamic Properties of ordinary Water Substance for General and Scientific Use). Experimental data for conductivity at such superheating temperatures under atmospheric pressure may also not be available for a selected electrolytic solution. It can here be preferred to fit electrical conductivity to experimentally measured

conductance curve. The higher concentration of salt in the electrolytic solution, the higher the conductivity, and accordingly, the lower the applied voltage that is required to reach a selected pore temperature.

[0030] With this framework in place, the geometric conditions of the physical pore system can be imposed to determine the heating control of a given pore geometry. An example of pore geometry boundary specification is shown in Figure 3. The support structure 12 is here given as a membrane having a thickness, t, at the site of the pore that is the length of the pore. The pore is specified with a radius, r. The system is specified as having an external boundary, S, that is set as some reasonable value, such as 200 microns, with an axisymmetric boundary, an opposing boundary at which the normal current density is set as zero, by specifying $\boldsymbol{\eta} \cdot \boldsymbol{J}=0$. There is defined a boundary at which a voltage source is applied, and an opposing boundary at which the voltage is zero, $V=0$.

[0031] With the pore geometry conditions and electrolytic solution conditions in place, the heating of electrolytic solution in the pore as a function of applied voltage across the pore can be determined for enabling precise control of the heating in the pore. Referring to the plot of Figure 4, there are shown results for one example in which the system is specified as a pore in a Si_3N_4 membrane with an electrolytic solution of 3 M NaCl provided in the *cis* and *trans* fluidic chambers. Fig. 4 is a plot of internal pore temperature that is determined by the modeling method as a function of applied voltage for five different pore geometries. This plot demonstrates that when the pore radius, r, is on the order of the pore length, which is the membrane thickness, t, there is a fixed relationship between pore temperature and applied voltage. In other words, for any pore in which the pore length is about the same as the pore radius, then the same temperature will be produced in the pore for a given applied voltage, no matter the pore radius, over a range of tens of nanometers. Thus if the value of the pore radius and the value of the pore length are within about ten nanometers of each other, then the same temperature will be

achieved for a given voltage, for any pore radius. As the thickness of the membrane is increased beyond the pore radius value by more than about ten nanometers, the dependence between temperature and applied voltage changes, and is different for different aspect ratio pores.

[0032] The plot of Fig. 4 includes a horizontal dashed line that represents the threshold temperature for superheating a 3 M NaCl solution in the model just described. For any temperature above this threshold temperature, superheating of the solution in the pore is obtained. As explained above, any temperature above the equilibrium boiling point of a given liquid is a condition of superheating the liquid. Thus for any selected pore system geometry, and knowing the threshold superheating temperature for a given electrolytic solution, the voltage to be applied across the pore can be determined for obtaining superheating within the pore. For example, for the pore system conditions corresponding to the plot of Fig. 4, for a pore having a 50 nm radius and a 100 nm-long pore in a membrane, an applied voltage of about 6 V is required to obtain superheating of a 3 M NaCl electrolytic solution in the pore.

[0033] With superheating conditions produced within the pore, there can be conducted experiments and analysis on species that are provided in the fluidic chambers, and on species held in the pore itself. For example, there can be conducted reactions between liquids and species in the two chambers at the pore. In one embodiment, the electrolytic solution in the pore is controlled to be in a state of superheating and species in the pore react in the high-temperature environment there. Thus the pore and fluidic chambers provide an apparatus for inducing and studying chemical phenomena in the vicinity of the pore. Indeed the manufacture of chemicals requiring superheated solvents can be facilitated or affected by the use of such solid state pores, either individually, in small arrays, or in massive arrays. The apparatus thereby provides a bubble-reaction chamber in which high-temperature reactions can be conducted.

[0001] Figure 5 is a thermal plot of the temperature across a 53.5 nm-radius, 71 nm-long pore when a voltage pulse of 8.22 V is applied for 10.4 μs across the pore. Note that the temperature exhibits a thermal profile across the pore in which the highest temperature is at the center of the pore, with a temperature of 600K, while the temperature at the wall of the pore is 470K. Thus, in the metastable superheating state, the nanopore exhibits a thermal profile in which the temperature at the center of the nanopore may be much higher than the threshold temperature for superheating. When the electrolytic solution in the nanopore reaches an extreme level of superheat, the solution can approach the temperature limit of superheating. This temperature limit is defined as the temperature beyond which the liquid is thermodynamically unstable and must vaporize.

[0034] In one embodiment provided herein, as the temperature of the electrolytic solution in the nanopore approaches the temperature limit of superheating, there can be controlled the nucleation of homogeneous vapor-phase bubbles in the nanopore. Referring again to Figure 2A and also to Figure 2B, as the focused electrolytic solution causes Joule heating in and near the pore, with a thermal profile like that of Figure 5, in which the highest temperature is reached at the center of the pore, then as shown in Figure 2B, a vapor bubble can homogeneously nucleate. Here 'homogeneous bubble nucleation' refers to bubble nucleation at a location in the pore cross section that is not at the wall or surface of the pore or support structure and instead is away from the wall of the pore, and can be toward the center of the pore cross section, in the liquid. This is in contrast to heterogeneous bubble nucleation in which a bubble forms at a surface. Rapid Joule heating of the electrolytic solution as provided herein can be controlled to cause the homogeneous nucleation of a bubble within the pore.

[0035] From a thermodynamic standpoint, a vapor bubble could form in the pore at any time when the temperature of the electrolyte in the pore has been elevated above the equilibrium boiling point of the electrolyte. But in

actuality, one would need to wait for a very, very long time, beyond reasonable experimental timescales, for a bubble to form if the temperature of the electrolyte is superheated but significantly less than the temperature limit of superheating of the electrolyte. In contrast, if the temperature of the electrolyte is superheated and controlled to approach the limit of superheating, then a vapor bubble can be caused to form almost instantaneously in the pore. This is governed by the kinetic rate of the process, as explained in, e.g., in Blander, M. and Katz, J. L. (1975), Bubble nucleation in liquids. AIChE J., 21: 833–848.

[0036] Thus, there can be produced controlled homogeneous bubble nucleation, and a sequence of bubbles, in a pore, away from the pore wall, by applying across the pore a voltage bias that causes the electrolyte in the pore to be superheated to a temperature approaching the limit of superheat of the solution. For example, for a 3 M KCl solution, the temperature of the electrolyte must be above about 550 K in order for a bubble to homogeneously nucleate within a reasonable amount of time. Thus, for a 100 nm-diameter, 100 nm-long pore, as represented in the plot of Fig. 4, an applied voltage of at least about 8 V is required to controllably initiate homogeneous bubble nucleation.

[0037] The temperature profile across a pore indicates that the localized temperature maximum at the pore center dramatically increases the likelihood that a bubble will nucleate homogeneously there. This is demonstrated with the plotted data of Figure 6, which is a plot of the calculated nucleation rate of as a function of distance from the center of the pore. This data corresponds to the pore conditions of 53.5 nm in radius and 71 nm in length, with application of 8.22 V across the pore, with surface tension of the liquid-vapor interface taken to be that along the saturation curve. The rate is sharply peaked at the cross-sectional center of the pore, supporting homogeneous single bubble nucleation at the pore center.

[0038] As a homogeneously nucleated vapor bubble expands outward from the center of the pore, across the cross section of the pore, the bubble cuts off the Joule heating of the electrolytic fluid when the bubble reaches the pore periphery at the edge of the pore support structure. The bubble then continues to grow due to fluid inertia and thermal energy that is stored in the superheated electrolytic fluid. The bubble ultimately reaches a maximum size and then collapses when the vapor pressure in the bubble decreases below the ambient pressure in the liquid. Thus, after nucleation, the bubble grows at the pore, with a bubble surface that can extend completely across the cross-section of the pore, thereby effectively completely blocking ionic current flow through the pore between the two fluidic chambers. To further increase the likelihood of bubble formation at the center of the pore cross section, it is preferred that the membrane or other pore support structure be provided as a material that has a relatively high thermal conductivity and wettability. This condition aids in maintaining the temperature of both the pore walls and the fluid in the pore at the periphery of the pore, near the walls, lower than that of the fluid at the center of the pore. As a result, a temperature profile with a higher central temperature can be achieved at the center of the pore and homogeneous bubble nucleation can be controllably initiated at the center of the pore. This in turn enables bubble growth across the pore, to completely fill the cross-sectional diameter of the pore.

[0039] This vapor bubble formation thereby results in a drop or even complete blockage in ionic current flow through the pore, with a corresponding drop in electrical current through the circuit to which the pore system is electrically connected. As a result, the presence of a bubble filling the cross section of a pore can be detected by discontinuous current flow. Figure 7 is an example plot of ionic current flow through a pore as a function of time. As a bubble homogeneously nucleates in the pore and expands across the pore to block current flow through the pore, the presence and absence of a bubble in the pore can be determined by the level of measured current through the circuit.

[0040] In one embodiment, to reliably control homogeneous bubble nucleation in the pore, the applied voltage is set to that voltage which causes superheating of the electrolytic fluid in the pore to a temperature that is e.g., about 10°, about 5°, or about 1° less than the temperature limit of superheating at which bubbles would form. Then there can be injected into the electrolytic fluid additional energy that initiates the nucleation of a bubble. This additional energy can be applied by, e.g., raising the voltage applied across the pore, e.g., as in a pulsed fashion, by directing a beam of energy, such as a laser beam, at the pore, or by chemical reaction at or near the pore. In one methodology, the temperature of the electrolyte in the pore is raised from superheating to about the temperature limit of superheating, where bubbles will form, to controllably initiate the homogeneous nucleation of vapor bubbles in the pore by introducing additional energy to the pore. Once this condition is set, vapor bubbles will sequentially nucleate, expand, and collapse in the pore with a fixed regularity.

[0041] Bubble nucleation can also be initiated at the pore by the transfer of energy from an object that is at or in the pore to the fluid in the pore to approach the temperature limit of superheating conditions for initiation homogeneous nucleation of a bubble in the pore. This energy to be transferred from the object can be imparted to the object by any suitable means, e.g., by an energy source that is external to the pore system. For example, optical energy from a laser source, chemical energy resulting from, e.g., a chemical reaction of an object or objects in the pore, or other scenario can be employed to deliver energy to an object for transfer of a highly-localized heat pulse to the liquid at the pore.

[0042] In one example methodology, the temperature of the electrolytic liquid in the vicinity of the pore is controlled to be above the known superheating temperature of the liquid and less than the temperature limit of superheating, e.g., by ten degrees, less than the temperature limit of superheating by five degrees, or less than the temperature limit of

superheating by one degree. The fluid electrolytic liquid in the pore and vicinity is heated by Joule heating of the electrolytic solution as the solution and ionic current is focused through the pore. For a selected electrolytic solution, pore support structure material composition, pore radius, and pore length, there is determined the voltage to be applied across the pore, between the two fluidic chambers, to obtain this thermal condition in the pore. The quantitative analytical modeling detailed above, e.g., using the COMSOL MultiPhysics program, from COMSOL, Inc., Burlington, MA, or other suitable technique, can be employed to determine the requisite voltage to be applied across the pore. The electrical voltage in the circuit 24 in Figure 1 is thereby controlled so that with the voltage applied by the electrodes at each fluidic chamber, the liquid at the pore is at or just below, by less than one degree, less than five degrees, or less than ten degrees, the temperature at which bubbles would homogeneously nucleate at the pore in a reasonable time period.

[0043] Now referring to the schematic system view of Figure 8, external energy is directed to an object at the pore for absorption of the energy by the object. Once absorbed, the object releases the absorbed energy, transferring the energy from the object to the surrounding liquid. This energy transfer causes homogeneous bubble nucleation at the pore under the conditions that the liquid is thermally biased at a condition of superheating as given above. As shown in Figure 8, in one embodiment, there is configured a laser 45 or other source for directing an energetic beam, such as a laser beam 47, toward the pore so that when an object 15 is at the pore, the object is irradiated with the energy beam. In one embodiment, the energy beam characteristics are controlled to be complimentary with that of an object of interest, so that the selected object is capable of absorbing the energy of the beam. The excitation energy absorbed by the object is then transferred 50 from the object to the fluid at the site of the object, e.g., by thermal heat transfer. This energy transfer triggers homogeneous bubble nucleation 25 at the pore by raising the temperature of the liquid in response to the energy transfer. As just explained, in this methodology, the temperature of the fluid is quiescently

controlled, i.e., thermally biased, by selection of voltage conditions, to be superheated and just below the superheating limit temperature, so that the radiative fluid heating by the object initiates bubble formation at the pore.

[0044] In one embodiment, the absorption line of an object of interest is determined and a beam of light having an energy corresponding to that absorption line is directed to the pore. When the object of interest is at the pore, the object will absorb the energy from the beam. Objects not having that absorption line will not absorb the energy from the beam. Once the beam energy is absorbed by the object, the object radiatively releases the absorbed energy, and transfers this energy to the fluid in the vicinity of the object at the pore by heating the fluid. The temperature of the fluid is thermally biased just below the critical temperature for bubble formation, so that the radiative fluid heating by the object can initiate bubble formation at the pore. Thereby, the formation of a bubble by a selected object, such as a selected molecule or class of molecules, can be controllably imposed by an external excitation that is specific to a molecule of interest.

[0045] Similarly, a highly localized heat pulse can be transferred from an object to the liquid by a chemical reaction that is specific to a particular object or class of objects. A reactive species or chemical can be disposed at the membrane surface, on the pore walls, or otherwise disposed in the vicinity of the pore, or provided in the second fluidic chamber opposite that including an object to be detected. When the object interacts with the reactive species, the energy of the chemical reaction can heat the fluid in the vicinity of the pore to form a bubble at the pore.

[0046] As shown in Figure 9, when an object 15 is in the pore 18, and homogeneous bubble nucleation has been initiated, the bubble expands and can extend completely across the cross section of the pore. When the bubble completely fills the pore in this manner, then the level of electrical current, *I*, in the circuit 24 in Figure 1 reflects the presence of the bubble and presence of the companion object in the pore, with the current effectively completely

blocked by the bubble extension completely across the pore. Thus, because a bubble can completely fill the cross-section of the pore, the presence of the companion object at the pore can be very effectively detected even if the object is nonuniform and/or smaller in diameter than the pore. In other words, for any object diameter, the bubble provides the ability to completely block ionic current flow, and corresponding electrical current flow. The measured signal in the current is therefore a robust and reproducible mechanism for detecting a wide range of objects in the pore.

[0047] Thus, as objects translocate through the pore, entering the pore and exiting the pore, the level of electrical current flow through the closed-loop circuit reflects the formation of vapor bubbles due to this sequence of object translocation. The measured circuit current flow reflects the presence of a bubble at the pore, and indirectly reflects the corresponding presence of an object in the pore that caused the formation of the bubble. The measurement of the current through the circuit thereby enables electronic detection of the presence of an object at and/or in the pore, indirectly, via the reduction or cut off of ionic current due to bubble formation.

[0048] The indirect detection of the presence of an object in the pore can be accomplished by means other than electronic, and electronic measurement is not an absolute requirement for the pore-based sensing system. All that is required is a detection of a bubble at the pore when a companion object or objects are at the pore. Other detection mechanisms can be employed. For example detection can be optical, by interaction of a bubble and/or companion object with an external light beam. In this scenario, as shown in Figure 10, a light source 30 can be positioned to direct an external optical beam 32 toward the pore so that when a bubble 25 is present at the pore, a reflection 34 of the beam off of the bubble surface can be detected at an optical detector 36. Similarly, optical transmission through the pore can be monitored with an optical beam directed through the pore, with a drop in optical transmission

through the pore indicating the presence of a bubble. Alternatively, referring to Figure 11, the sound waves 38 that are formed in the solutions in the fluidic chambers by bubble nucleation and formation can be detected by acoustic detectors, such as ultrasound detectors, or microphones. Similarly, a MEMs-based flow sensor near the pore can make such a detection. These examples demonstrate that bubble detection can be accomplished by any in a wide range of techniques. Other detection technique can be employed separately or in conjunction with an electronic detection technique.

[0049] Turning to considerations for the pore structure, the pore support structure, and electrical biasing are all selected to obtain controlled superheating conditions. The support structure can be implemented as a substrate, chip, suspended layer, membrane, or other structure in which a generally microscale-to-nanoscale length of a pore can be achieved between two surfaces of the structure separating the *cis* and *trans* chambers. The structure can be electrically insulating, conducting, or semiconducting, but if electrically conducting, it can be preferred to coat the structure with an electrically insulating layer or layers. For many applications, it can be preferred that the pore be formed in a solid state support structure such as a solid state membrane; a biological membrane or combination of solid state and biological structures can also be employed. A solid state membrane can be formed of any suitable material, such as silicon nitride or silicon dioxide, or other electrically insulating, wettable, and thermally conducting material or composite of a plurality of materials. A microelectronic membrane is particularly well-suited as a pore support structure. Herein the term "membrane" refers to a generally thin layer of material that is self-supported across its extent and is supported at its edges by, e.g., a structural frame such as a substrate. The support structure thickness can be a suitable thickness for supporting the pore, e.g., about 1000 nanometers in thickness or less, and can include or be formed of atomically thin materials such as graphene and other such materials. The *cis* and *trans* chambers can be provided in concert with the support structure as flow channels, fluidic

inlets and outlets or ports, or other fluidic structures, for enabling delivery of a fluid in a chamber to or from a pore for translocation of species in the fluid through the pore.

[0050] The pore can be any suitable diameter, e.g., 1 micron or less, e.g., 150 nanometers or less, 100 nanometers or less, 50 nanometers or less, or 10 nanometers or less. Biological pores can be employed as-suitable for a given application. For example, the toxin produced by the bacterium *S. aureus* is a protein called α-hemolysin. Monomers of this protein in an aqueous solution self-assemble into lipid bilayers, or into cell membranes, as a heptamer that creates an aqueous channel or pore of diameter ~1.5 nm through the lipid bilayer. Other biological pore arrangements can be employed.

[0051] A pore can be formed in a selected solid state support structure by any convenient process, e.g., by ion beam milling, electron beam milling, ion beam sculpting, wet or dry etching, or other selected process. The support structure for the pore, as well as electrodes, contact pads, and connections, can be fabricated in any suitable manner as-desired for a given molecular detection application. Fabrication processes for producing microelectronic membranes and for producing pores in such membranes with associated electronic connections can be implemented in a manner best-suited for a given application, as, e.g., in U.S. No. 6,783,643, issued August 31, 2004; U.S. No. 6,627,067, issued September 30, 2003; U.S. No. 7,258,838, issued August 21, 2007; U.S. No. 6,464,842, issued October 15, 2002; U.S. No. 7,582,490, issued September 1, 2009; U.S. No. 7,468,271, issued December 23, 2008; U.S. No. 7,118,657, issued October 10, 2006; U.S. No. 8,206,568, issued June 26, 2012; and U.S. No. 8,273,532, issued September 25, 2012; the entirety of each of which is hereby incorporated by reference.

[0052] The fluidic chambers are provided with a suitable electrolytic solution for producing an ionic flow through the pore and for transporting species through the pore. An example of suitable electrolytic fluid is a solution of water and a salt, with a salt composition and

concentration such as 3 M KCl. The electrodes can be provided in contact with the solution as, e.g., silver-silver chloride electrodes in the fluidic chambers in the conventional manner. With this configuration, an applied voltage across the membrane of any suitable magnitude, e.g., between about 1 V and about 20 V, or between about 5 V and about 10 V, can be imposed, with an electrical current flow of ~ 30 μA. Alternatively, a current source can be included in a circuit that connects that pore in series with the current source, between the two fluidic chambers, to control the current through the pore for Joule heating of the electrolytic fluid in the pore.

[0053] Methodology is further provided herein for distinctly identifying objects translocating through the pore. It is recognized that homogeneous bubble nucleation is initiated for different species of objects at different levels of fluid superheating. Therefore, for a given fluid temperature, superheating and bubble formation occur for a corresponding object having attributes that correspond to the temperature at which the fluid is controlled. A drop in circuit current thereby corresponds to a given fluid temperature for a particular object and object geometry. The circuit bias can therefore be set for a given selected object, such as a molecule, a class of molecules, or a particular species or group of species, for detection of that particular selected molecule, class of molecule, or species, by detection of bubbles that form in the pore for the given circuit bias.

[0054] In addition, an array of pores can be employed, one pore for each distinct object or class of objects. Each pore in the array can be biased at selected conditions for bubble formation and circuit detection of one corresponding distinct object or class of objects. In this scenario, the array of pores provides complete detection of any number of selected distinct objects, such as the four distinct DNA bases.

[0055] These examples demonstrate that the bubble nucleation methodology herein can be tailored to impose object-specific control on bubble nucleation. Thereby, the formation of a bubble and its detection can be

directly correlated to a specific object for which the bubble nucleation control is tailored. Any suitable objects, species, particles, and organisms can be provided in a fluidic chamber of the bubble formation system for detection by the system, including both naturally occurring and synthetic molecules. Biomolecules, e.g., polymers including nucleic acids such as single-stranded or double-stranded DNA and RNA, proteins, polysaccharides, lipids, and synthetic polymers all are particularly well-addressed by the detection system. The object can also consist of one or more portions of a full molecule, e.g., a component of a molecule such as an oligonucleotide or sequence of DNA bases. The objects to be included in a fluidic chamber liquid are thus not limited to a specific molecule, species, or component of a molecule. Correspondingly, the cross-sectional geometry of the pore is not limited to a particular extent or shape, and can be tailored to accommodate objects or species of interest.

[0056] It is recognized that the index of refraction of the liquid in the chambers, in the vicinity of the pore, can be modulated by adjusting the ionic current flowing through the pore. One effect contributing to this phenomenon is the temperature dependence of the index of refraction of the liquid near the pore. This has the effect of deflecting or scattering light beams that pass in the vicinity of the solid state pore. Therefore, by controlling the Joule heating of the liquid at the pore, and by bubble formation at the pore, the change in liquid temperature can be controlled to change the index of refraction of the liquid at the pore. Then, with an arrangement like shown than in Figure 10, with external optics, the control of voltage applied to the chamber electrodes enables the electronic adjustment of the index of refraction. The pore thereby can be operated as a tunable focusing element or lens with no moving parts.

Example I

[0057] Referring to Figure 12, there was constructed an experimental bubble formation chamber 60. A single pore 62 was fabricated with a focused ion beam machine in a free-standing silicon nitride membrane 64 affixed to a

silicon dioxide/silicon frame 66. Silicon nitride was chosen because it is highly wettable and has a higher thermal conductivity than electrolytes of interest, both of which conditions are important for extreme superheating, minimizing heterogeneous nucleation. This silicon nitride membrane was 71 nm thick. The pore was 53.5 nm in radius. The membrane was mounted in a fluidic cell in which the membrane separated two fluid chambers 68, 70 connected fluidically and electrically only through the pore 62. A 3 M NaCl solution prepared in deionized, degassed water was added to each chamber and contacted with Ag/AgCl electrodes 72, 74. A pulse generator 76, HP 8110A, from Hewlett Packard, a current sensing resistor 78, and a 500 MHz, high bandwidth oscilloscope 80 were connected in a circuit with the fluidic cell with a compensation circuit to minimize the effect of capacitance between the two fluidic chambers.

[0002] Voltage pulses of 11 μs in duration, and ranging in amplitude from 4 V to 8.22 V, with a 30 ns rise time, were applied to the electrodes with the fluidic chambers filled with solution. Figure 13A is a plot of the measured electrical conductance of the pore as a function of time during the voltage pulse application. The data were filtered at 13 MHz from 0 to 1 μs and 20 MHz from 1 to 10 μs by an eight-pole Bessel filter. The initial pore conductance was 1.15 μS, aside from an initial capacitance spike due to imperfect compensation, and increased with time and applied voltage to a value of 3.5 μS and a current density of 3.3×10^{9} A/m^2. This rise in conductivity was due to the time-dependent Joule heating of the electrolyte in and near the pore and the positive temperature dependence of electrolyte conductivities, which are strongly influenced by the temperature dependence of the water viscosity. The noise in the data belongs to the oscilloscope amplifiers.

[0003] Figure 13B shows the conductance data of Fig. 13A, with the time scale magnified and for the 8.22 V voltage amplitude application. The data were filtered at 200 MHz. The faded background line is the unfiltered measured conductance data. At 10.4 μs there is shown a significant drop in

pore conductance. This drop in pore conductance corresponds to the nucleation of a vapor bubble, and is represented by a rapid drop in conductance when the bubble blocks the ionic conduction through the pore. After the collapse of this bubble, it is shown in the plot that subsequent bubble events occurred with quasi-regular periodicity. The duration of each bubble event was approximately 16 ns, with 120 ns between events. The bubble formation behavior was that of a relaxation oscillator whose time constant is determined by thermal dynamics.

[0004] The behavior of this relaxation oscillator can be understood with a simple model of the heating and cooling dynamics at the pore. The initial 16 ns bubble event is given as cutting off ionic current. During this event lifetime, the maximum temperature in the pore is found to drop by about 200 K due to thermal diffusion. The time needed to reheat the pore center to 600 K once ionic current resumes is calculated to be approximately 120 ns. This corresponds well to the experimentally measured time to the second bubble of 117 ns. The dynamics of bubble growth in an unbounded, uniform temperature, superheated liquid have been well studied and such analysis can be applied here. Inertial effects govern early bubble growth, driven by the high vapor pressure inside the bubble. An initial radial growth velocity of 126 m/s at 600 K is here calculated, using the Rayleigh-Plesset theory, which applies to spherically symmetric, free expansion in an unconfined liquid. The presence of the pore walls decreases the calculated growth speed. Nevertheless, the result corresponds reasonably well to the measured velocity of 50m/sec obtained from the optical probing data. This inertial growth modeling does not include mass transfer at the boundary or heat transport effects. At high temperature, the surface tension is greatly diminished, decreasing its effect on early growth. The effects of heat transport are only manifest in later stages of bubble growth.

Example II

[0005] Figure 14A schematically depicts a second pore-based experimental setup, here employing a 1.9 μm-radius, 2.5 μm-thick pore in a silicon nitride membrane, designed for optically probing the onset and location of bubble nucleation in the pore. It was determined that larger-radius pores exhibit similar quasi-periodic bubble nucleation to that observed in the smaller 53.5 nm-radius pore of Example I, albeit with lower frequencies at comparable voltage bias. Optical transmission of a focused 514 nm, 0.5 mW, CW laser beam 84 through the pore was measured. A 60x water immersion objective lens was employed to bring the laser to a beam waist diameter of 350 nm. The transmitted optical beam was captured and brought to a focus with f=0.62 optics onto a 1 ns response time silicon photodiode, Thorlabs DET10A. The photodiode current was monitored simultaneously with the time-dependent electrical signal from the ionic current passing through the pore. For this experiment, the response time for the ionic current measurement was determined by the capacitance of the pore membrane. The lateral x-y position of the beam waist could be accurately moved to different positions across the pore with beam steering optics. The laser beam waist was positioned near to the pore center.

[0006] Figure 14B is a plot of both the electrical conductance and the photodiode current as a function of time as an 18 V, 22 μs pulse was applied across the pore. The conductance and current fell rapidly at the onset of a bubble nucleation event, stimulated by the voltage pulse application. At this voltage, bubble nucleation events consistently occurred 14 μs after the pulse was applied. With this data, there can be defined an event onset time for both the optical and ionic current signal to be the intercept of the pre-bubble current level with the extrapolated linear region of the current drop. These are labeled in the figure as t_i and t_p for the ionic and photodiode current, respectively.

[0007] The laser beam waist was then moved from the center of the pore to the periphery of the pore. Figure 14C is a plot of measured pore conductance and photodiode current with the new beam waist position. As shown in the plot, as a result of this move, there was a clear increase in the delay in t_p with respect to t_i. This suggests that the bubble was formed at the center of the pore, and as a result of its finite growth velocity there was a delay until the surface of the bubble scattered the incident laser beam at the pore periphery.

[0008] Figure 14D is a plot of the offset $\Delta t = t_p - t_i$ as a function of the laser position across the pore in two perpendicular directions. The points corresponding to the data in Figs. 14B and 14C are indicated in Fig. 14D. Each point contains ten measurements. The error bars show the standard deviations from the mean. The symmetry of the data around the pore center confirms that the bubble nucleation events were homogeneous and occurred at the center of the pore. The bubble radius growth velocity obtained from the slope of the data in the figure is 52.1±1.6 m/s for the y-axis scan and 49.2±1.7 m/s for the x-axis scan.

[0009] A straightforward interpretation of this data involves rapid Joule heating of the electrolyte in and near the pore that ultimately resulted in nucleation of a vapor bubble at the pore center. As a vapor bubble expanded, it cut off the Joule heating when the surface of the bubble reached the pore periphery. The bubble then continued to grow due to fluid inertia and thermal energy stored in the superheated liquid. The bubble ultimately reached a maximum size and then collapsed after the vapor pressure in the bubble decreased below ambient pressure in the liquid sufficiently to overcome the inertial forces of liquid expansion.

[0010] The coupled space- and time-dependent ionic current density and temperature fields in and near the pore prior to bubble formation can accordingly be determined. The time-dependent conductance of the pore was modeled for comparison with the experimental results. The nonlinear,

inhomogeneous heat equation with a Joule heating source term was solved for the pore geometry using the COMSOL MultiPhysics program, COMSOL, Inc., Burlington, MA. The temperature dependence of the heat capacity, thermal conductivity and density were taken to be those of superheated water at atmospheric pressure, given by the IAPWS-95 formulation. The temperature dependence of the electrical conductivity of 3M NaCl solution at atmospheric pressure was chosen to fit the experimental results by extrapolating measured high temperature data taken at pressures above atmospheric.

[0011] The resulting computed pore conductance curves are shown as the solid smooth curves in Fig. 13A. Excellent agreement was achieved with the experimental data with reasonable temperature dependent properties of the solution. The predicted temperature attained at the pore center after 10 μs for each voltage pulse is indicated in Figure 13A for each conductance curve.

[0058] With this description, there is herein provided apparatus and methodology that enable the controllable production and detection of vapor bubbles at a pore to achieve homogeneous, highly reproducible bubble formation and detection. A wide range of electrical, chemical, optical, fluidic, and acoustic phenomena can be excited and observed in the high field and extreme environment of a solid-state pore with this platform. The apparatus and methodology herein enable a wide range of applications for indirectly detecting and identifying objects at or in a pore by detecting vapor bubbles formed at the pore by such objects. The methodology further provides the ability to study reactions and optical and chemical phenomena in the fluidic environment of the pore. The objects can be biological molecules, polymer molecules, DNA, RNA, DNA and RNA fragments, single DNA bases, and other molecules and species.

[0059] It is recognized that those skilled in the art may make various modifications and additions to the embodiments described above without departing from the spirit and scope of the present contribution to the art. Accordingly, it is to be understood that the protection sought to be afforded

hereby should be deemed to extend to the subject matter claims and all equivalents thereof fairly within the scope of the invention.

[0060] We claim:

1. A method for detecting an object comprising:

translocating an object through a pore in a support structure from a first fluidic chamber containing an electrolytic solution including objects to be translocated through the pore to a second fluidic chamber containing the electrolytic solution for receiving an object that has translocated through the pore;

heating the electrolytic solution in the pore to a temperature that is at least a superheating temperature of the electrolytic solution in the pore and that is less than a temperature for homogeneous bubble nucleation in the electrolytic solution in the pore;

increasing energy in the electrolytic solution in the pore to at least a temperature for homogeneous bubble nucleation in the electrolytic solution in the pore when an object is in the pore to initiate homogeneous bubble nucleation in the pore; and

detecting a bubble in the pore to indicate presence of an object in the pore.

2. The method of claim 1 wherein increasing energy in the electrolytic solution in the pore comprises directing at the pore a beam of energy that energetically excites an object at the pore, causing homogeneous bubble formation at the pore.

3. The method of claim 2 wherein the beam of energy comprises a laser beam.

4. The method of claim 2 wherein the beam of energy comprises a laser beam having a wavelength that corresponds to an energy absorption characteristic of an object at the pore so that energy of the laser beam is absorbed by the object.

5. The method of claim 2 wherein the first fluidic chamber contains an electrolytic solution including first objects and second objects to be translocated through the pore, and wherein the beam of energy comprises a laser beam having a wavelength that corresponds to an energy absorption characteristic of the first objects and not the second objects, so that energy of the laser is absorbed by the first objects and not the second objects.

6. The method of claim 2 wherein the laser beam is directed to a cross-sectional center location of the pore.

7. The method of claim 1 wherein heating the electrolytic solution comprises applying an electrical voltage across the pore, between the first fluidic chamber and the second fluidic chamber, wherein the electrical voltage has a voltage magnitude that causes Joule heating of the electrolytic solution to at least the superheating temperature of the electrolytic solution.

8. The method of claim 7 wherein applying an electrical voltage across the pore, between the first fluidic chamber and the second fluidic chamber, comprises electrically contacting the electrolytic solution in a circuit that generates the electrical voltage applied across the pore.

9. The method of claim 1 wherein heating the electrolytic solution comprises connecting a current source in series with the pore in a circuit that controls current directed through the pore.

10. The method of claim 1 wherein detecting a vapor bubble 1 wherein heating the electrolytic solution comprises reacting an object in one of the first and second fluidic chambers with a reactive species at

the pore in a reaction that heats electrolytic fluid at the pore by energy from the reaction.

11. The method of claim 1 wherein detecting a bubble at the pore comprises detecting a reduction in ionic current flow through the pore between the first fluidic chamber and the second fluidic chamber.

12. The method of claim 1 wherein detecting a bubble at the pore comprises directing an optical beam to the pore and detecting reflection of the optical beam off of a surface of a bubble at the pore.

13. The method of claim 1 wherein detecting a vapor bubble at the pore comprises detecting in the electrolytic solution sound waves produced by homogeneous bubble formation at the pore.

14. The method claim 1 wherein the first fluidic chamber containing an electrolytic solution includes objects that are electrically charged objects, and wherein translocating an object through a pore comprises electrophoretically driving an electrically charged object through the pore from the first fluidic chamber to the second fluidic chamber by applying a voltage across the pore, between the two fluidic chambers, that is of sufficient amplitude to cause the electrically charged object to translocate through the pore.

15. The method of claim 1 wherein heating the electrolytic solution comprises applying a voltage between the two fluidic chambers that is of sufficient magnitude for superheating of the electrolytic solution in the pore to a temperature that is at least a superheating temperature of the electrolytic solution and that is less than about ten degrees below a temperature for homogeneous bubble nucleation in the electrolytic solution in the pore.

16. The method of claim 1 wherein heating the electrolytic solution comprises applying a voltage between the two fluidic chambers that is of sufficient magnitude for superheating of the electrolytic solution in the pore to a temperature that is at least a superheating temperature of the electrolytic solution and that is less than about five degrees below a temperature for homogeneous bubble nucleation in the electrolytic solution in the pore.

17. The method of claim 1 wherein heating the electrolytic solution comprises applying a voltage between the two fluidic chambers that is of sufficient magnitude for superheating of the electrolytic solution in the pore to a temperature that is at least a superheating temperature of the electrolytic solution and that is less than about one degree below a temperature for homogeneous bubble nucleation in the electrolytic solution in the pore.

18. A method for controllably forming homogeneous bubbles in a pore comprising:

providing a pore in a support structure with the pore connected between a first fluidic chamber containing an electrolytic solution and a second fluidic chamber containing the electrolytic solution, the pore providing a sole path of fluidic communication between the first and second fluidic chambers;

heating the electrolytic solution in the pore to a temperature that is at least a superheating temperature of the electrolytic solution in the pore and that is less than a temperature for homogeneous bubble nucleation in the electrolytic solution in the pore; and

increasing energy in the electrolytic solution in the pore to at least a temperature for homogeneous bubble nucleation in the electrolytic solution in the pore.

19. The method of claim 1 wherein increasing energy in the electrolytic solution in the pore comprises directing at the pore a beam of energy, causing homogeneous bubble formation at the pore.

20. The method of claim 18 further comprising detecting a bubble at the pore.

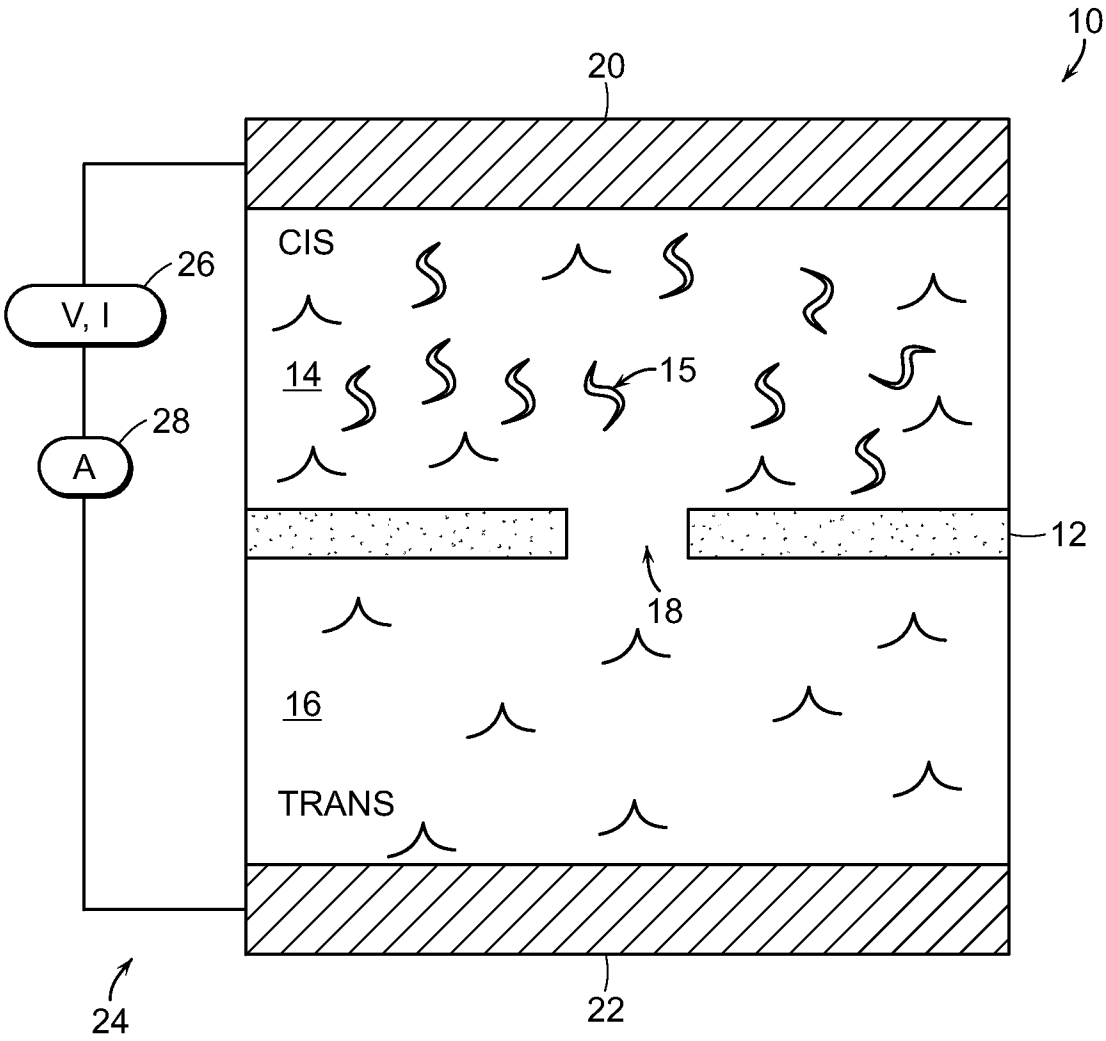


FIG. 1

FIG. 2A

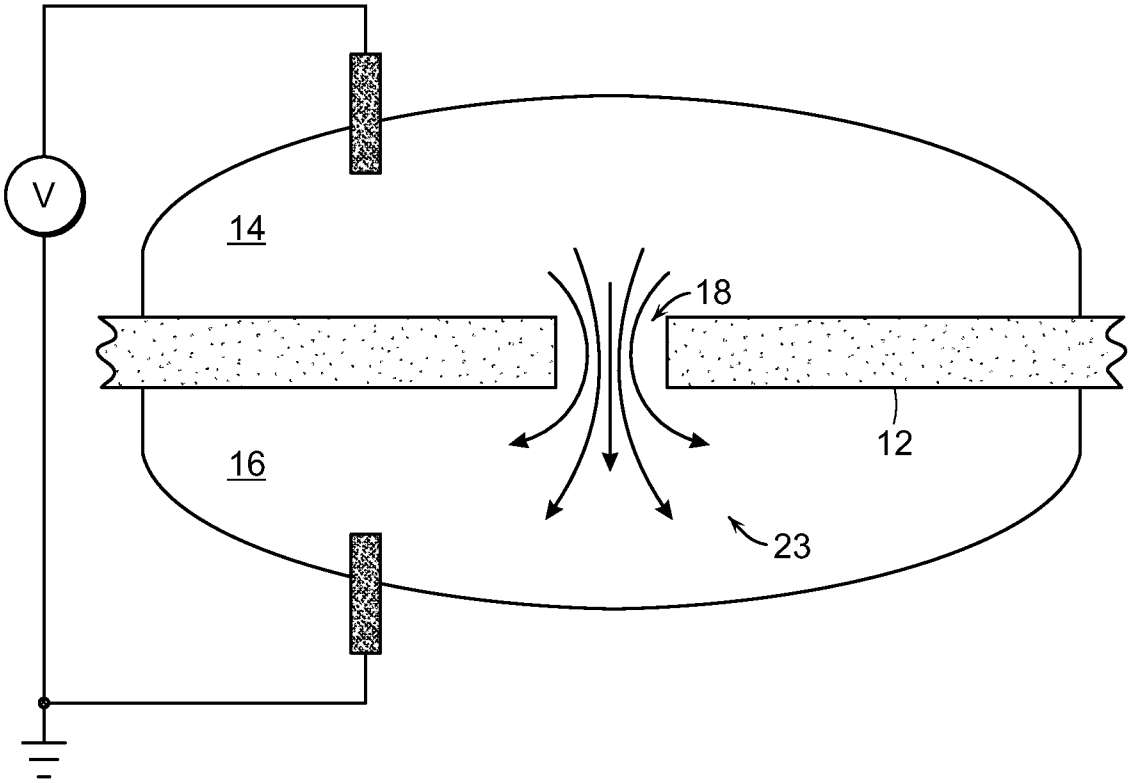
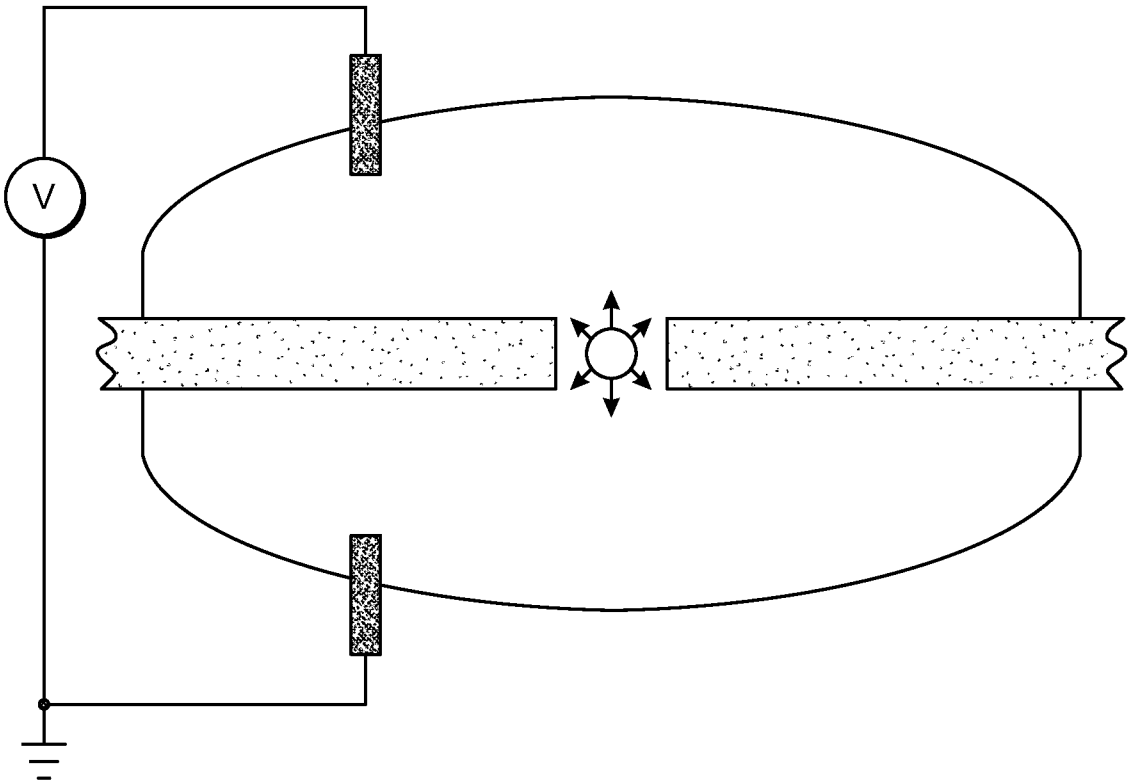


FIG. 2B



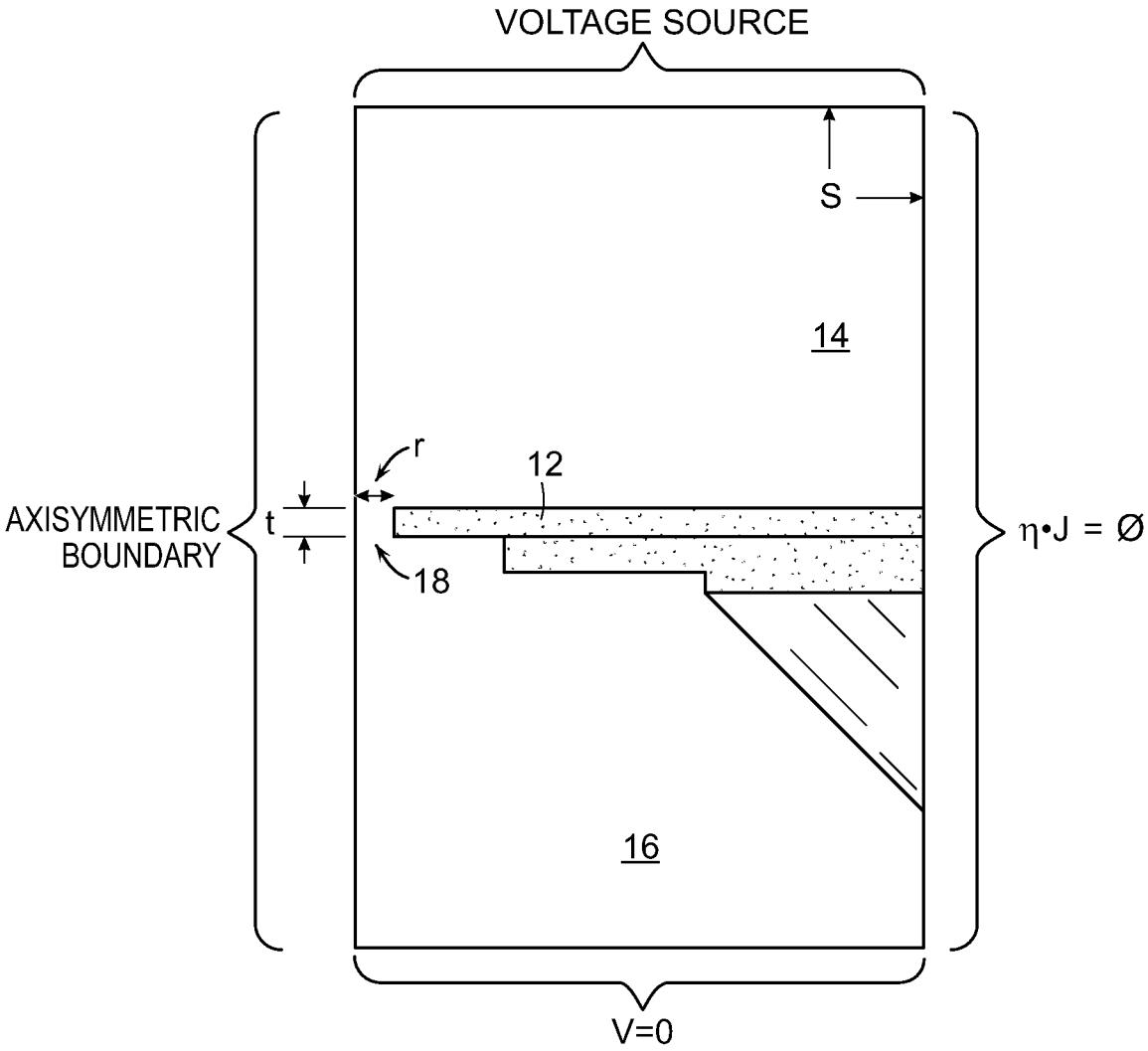
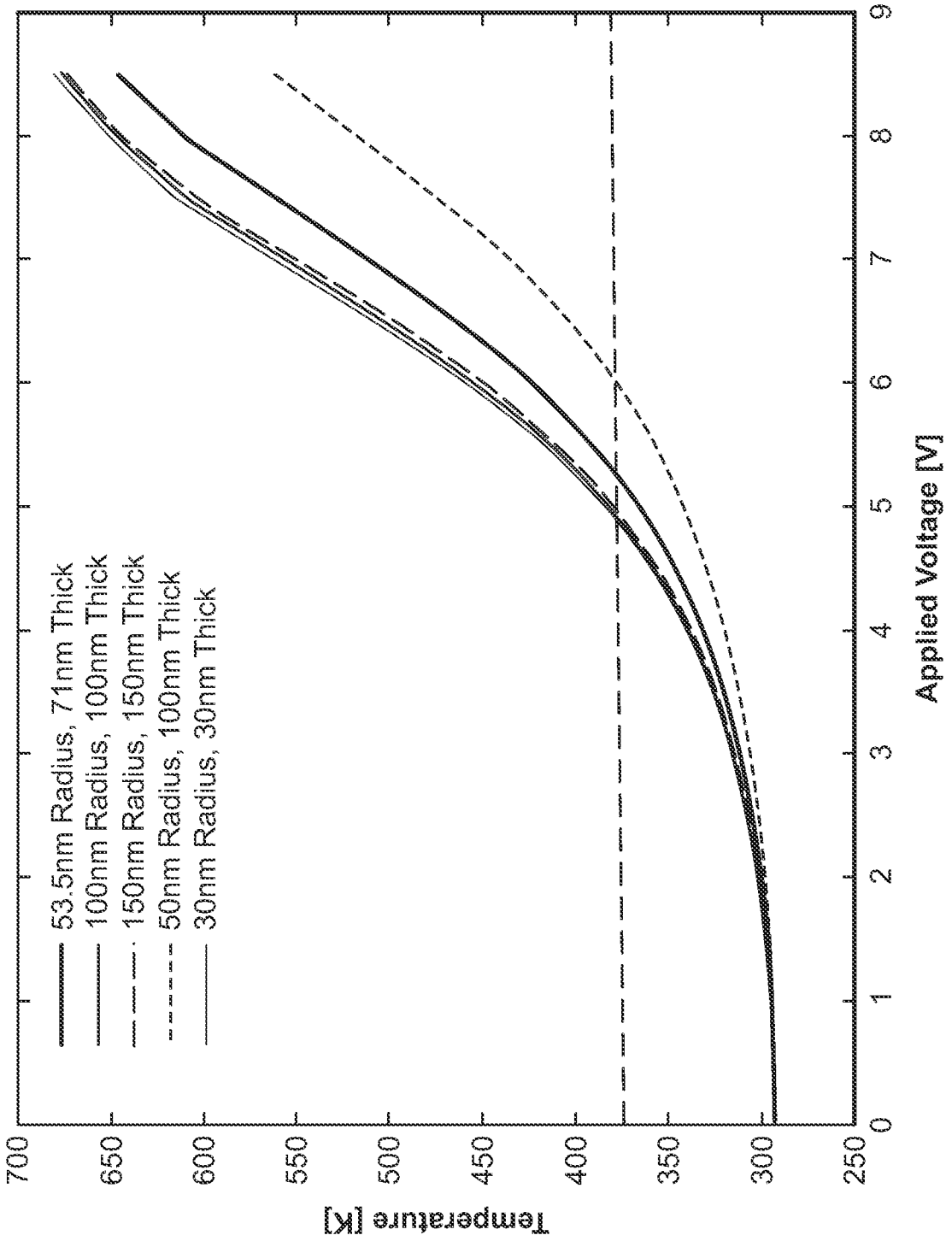


FIG. 3

FIG. 4


53.5nm Radius, 71nm Thick
100nm Radius, 100nm Thick
150nm Radius, 150nm Thick
50nm Radius, 100nm Thick
30nm Radius, 30nm Thick
Temperature [K]
Applied Voltage [V]
700
650
600
550
500
450
400
350
300
250
0
1
2
3
4
5
6
7
8
9

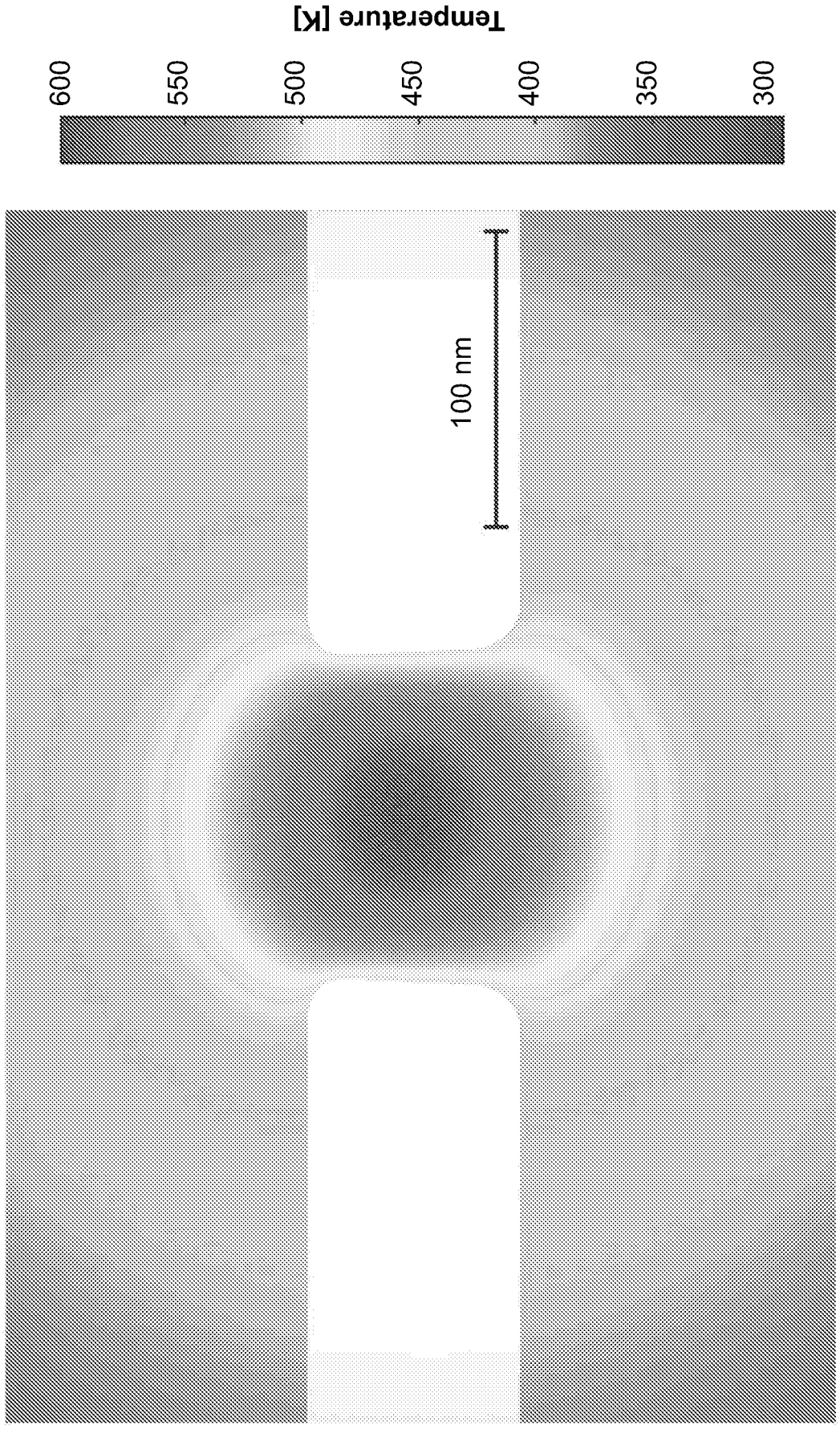


FIG. 5

FIG. 6

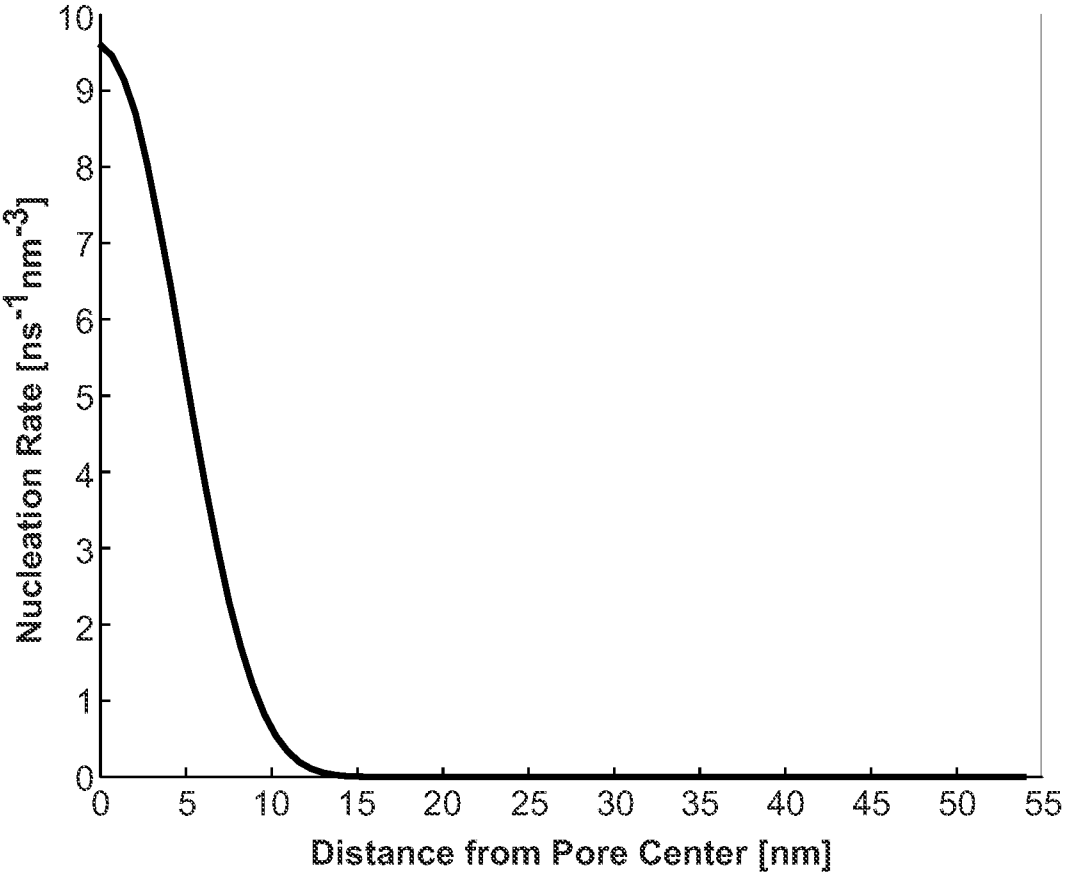

Nucleation Rate [ns^{-1}nm^{-3}]
0
1
2
3
4
5
6
7
8
9
10
0
5
10
15
20
25
30
35
40
45
50
55
Distance from Pore Center [nm]

FIG. 7

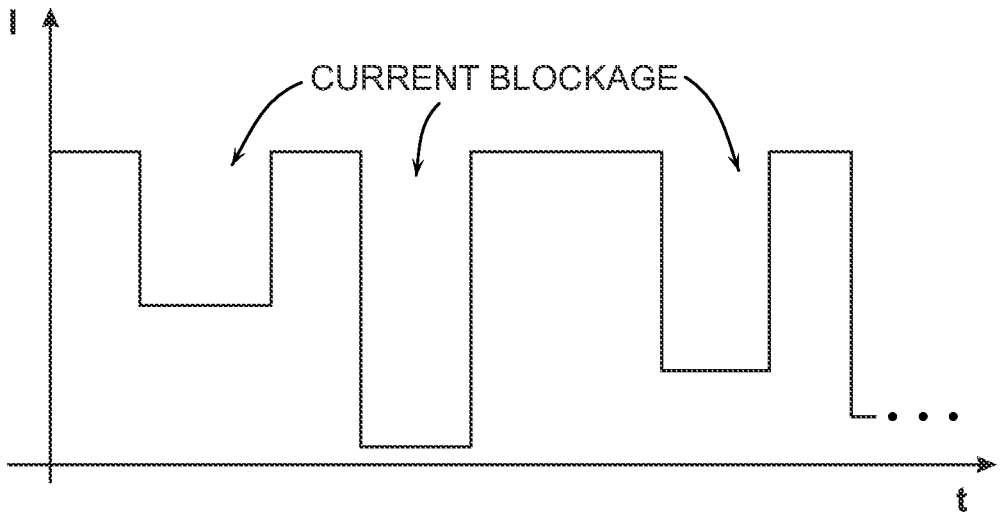

I
CURRENT BLOCKAGE
t

FIG. 8

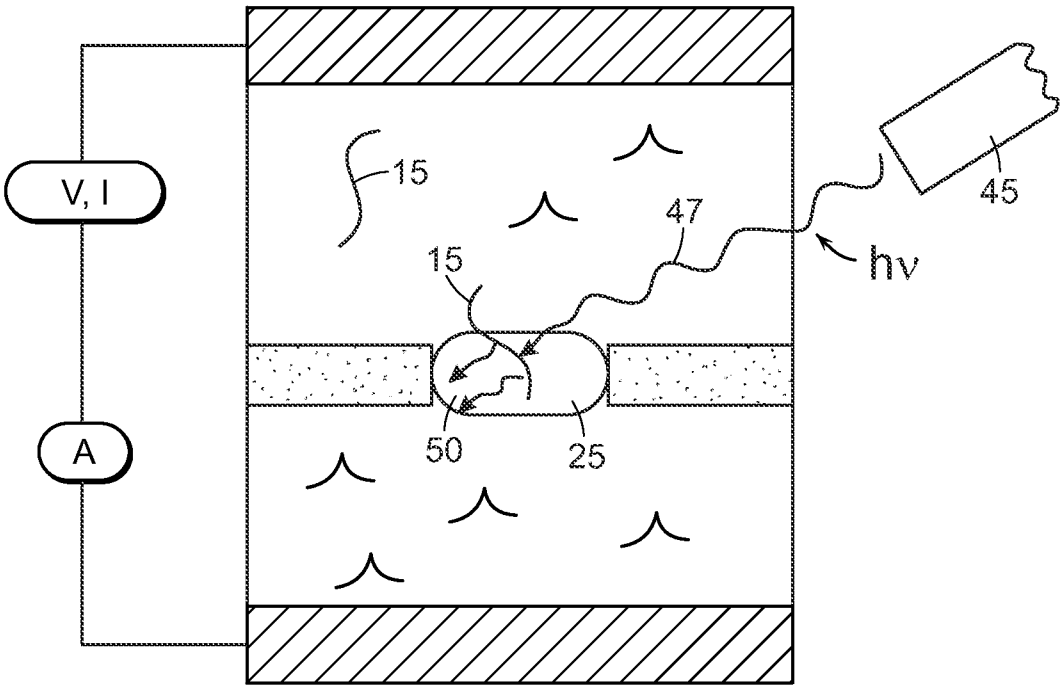


FIG. 9

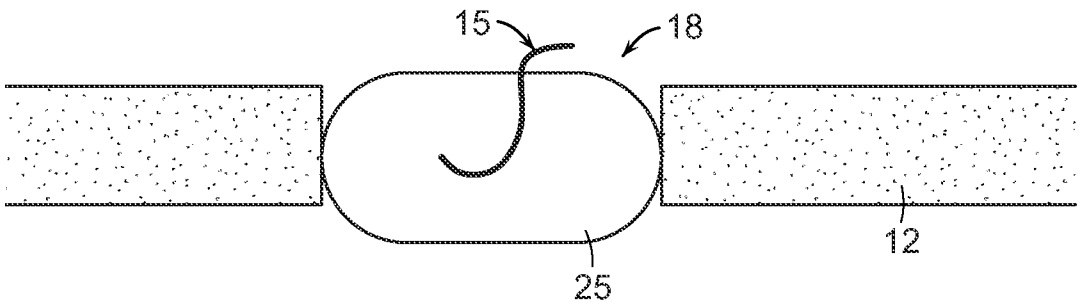


FIG. 10

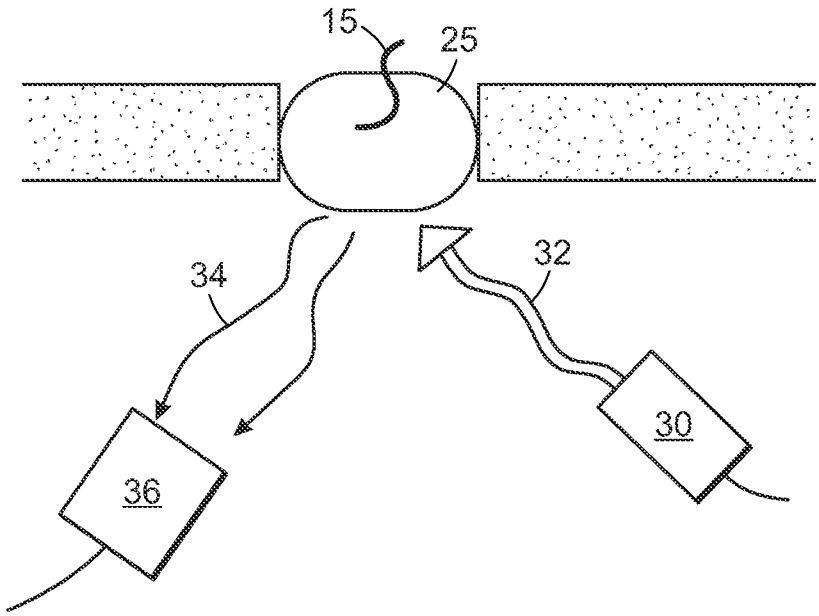
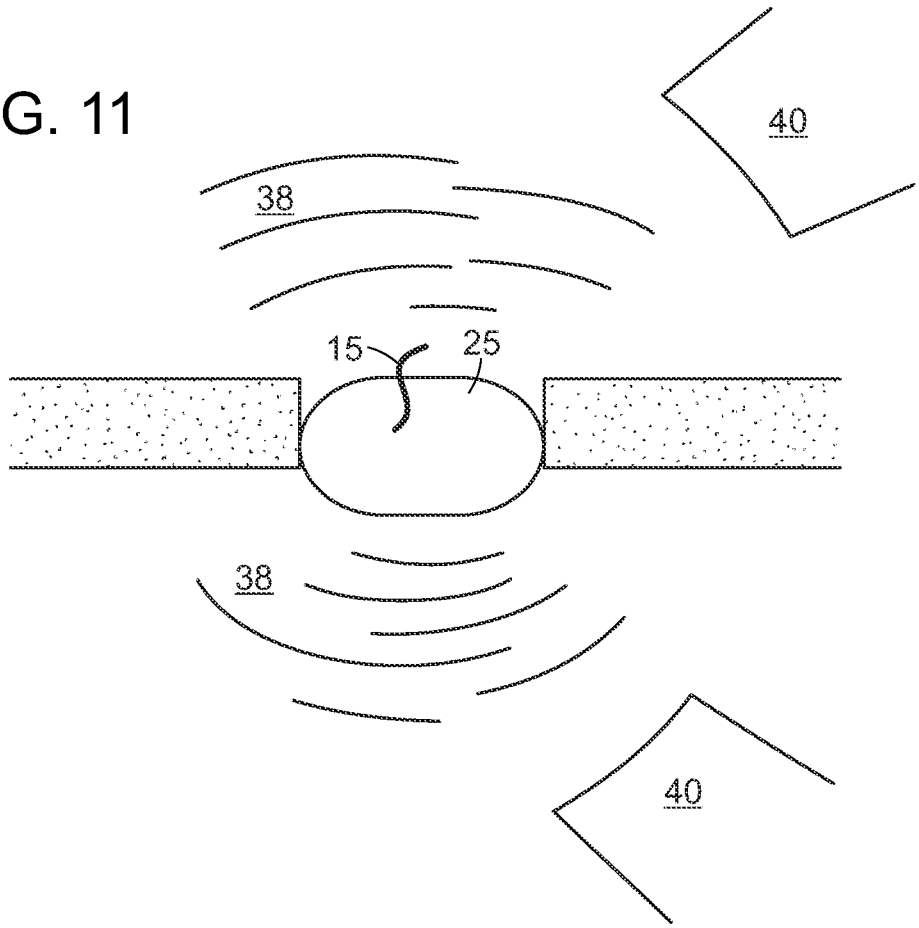


FIG. 11



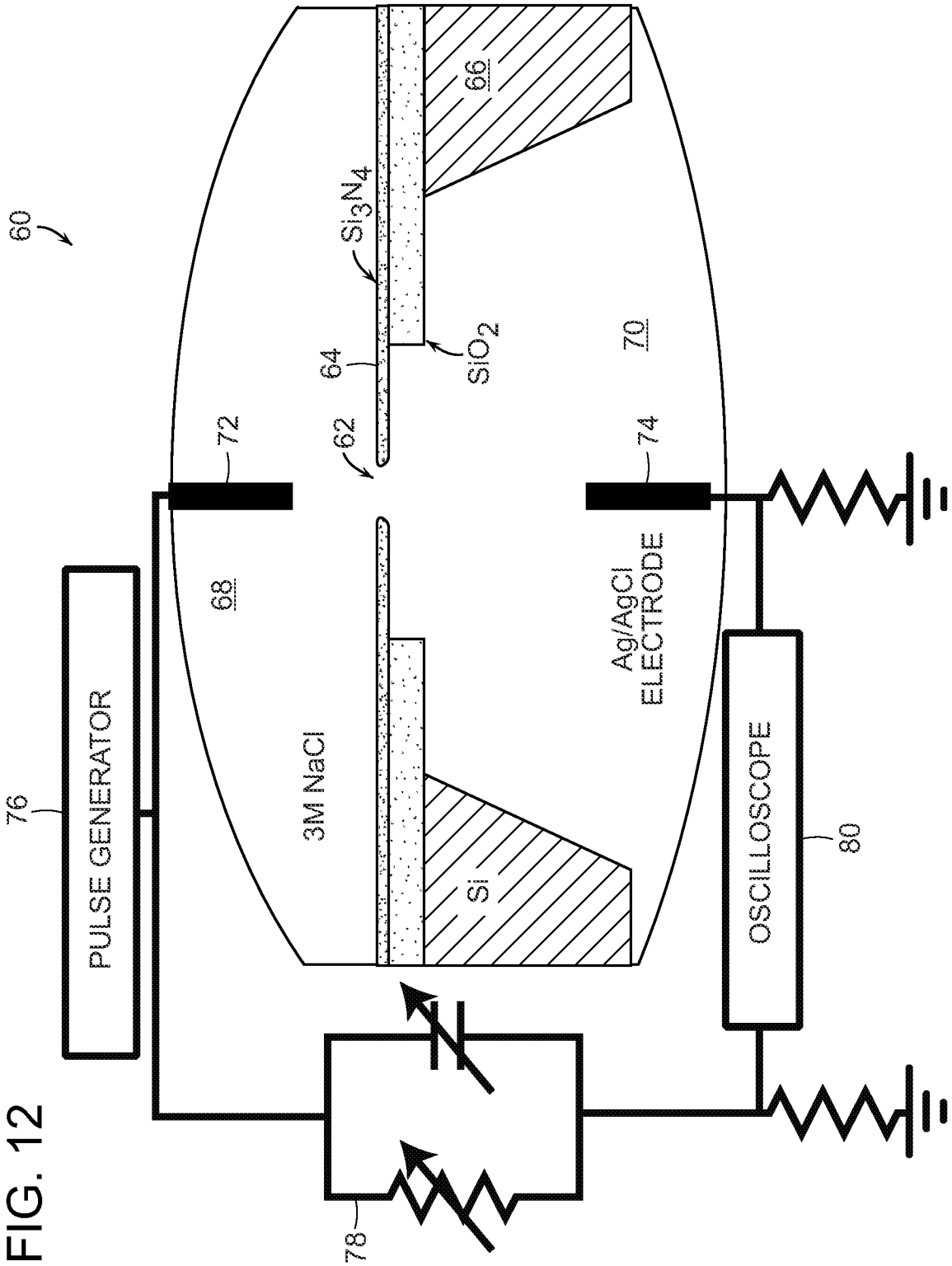

60
66
Si_3N_4
64
SiO_2
70
62
72
74
68
3M NaCl
Si
Ag/AgCl ELECTRODE
PULSE GENERATOR
76
OSCILLOSCOPE
80
78

FIG. 12

FIG. 13A

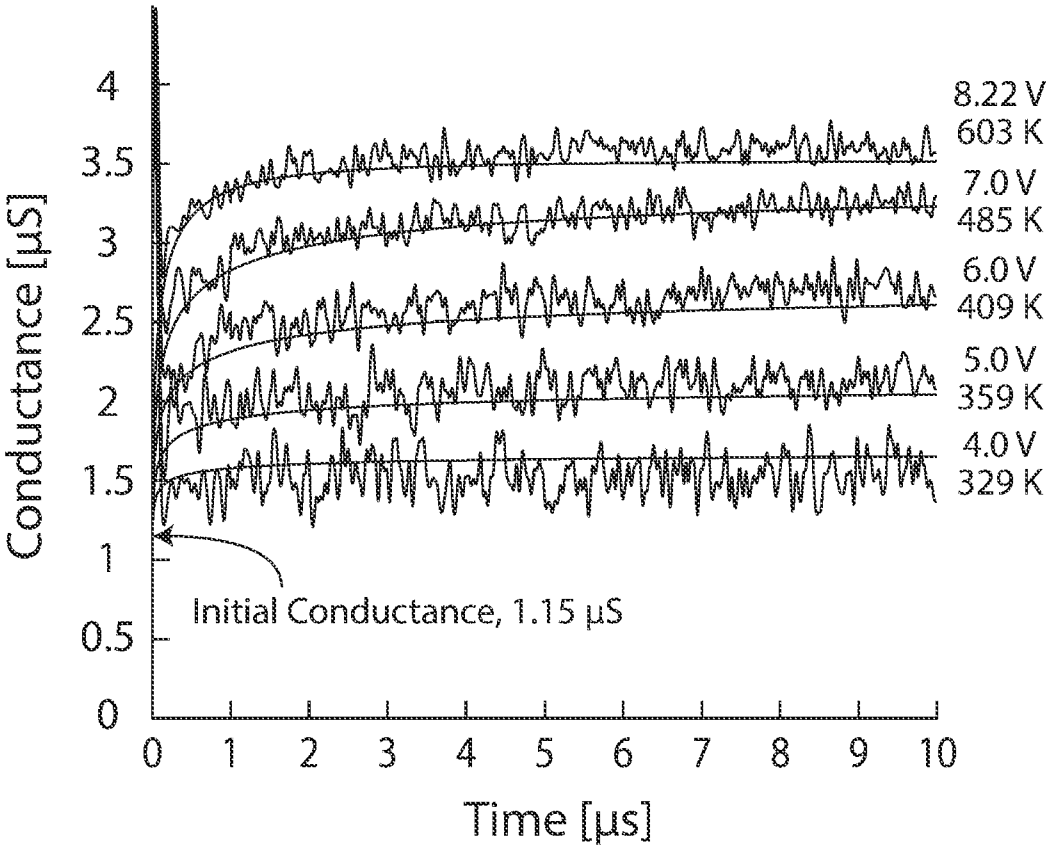


FIG. 13B

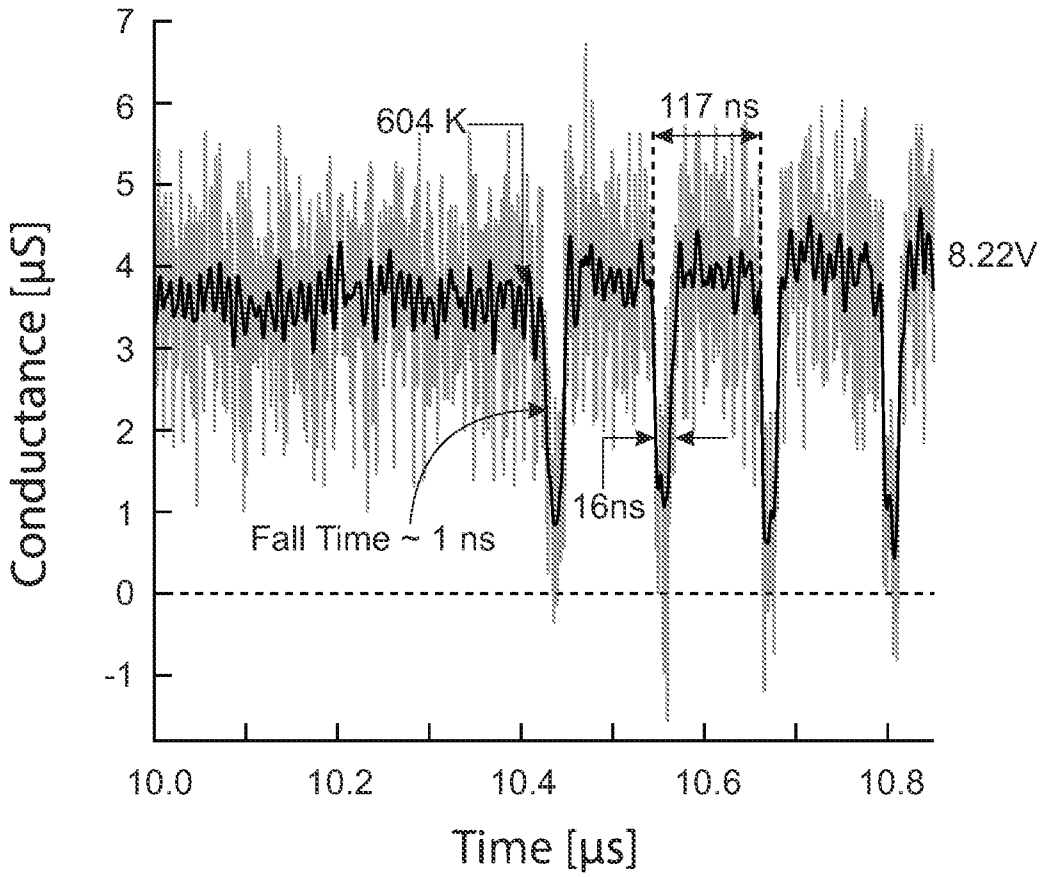


FIG. 14A

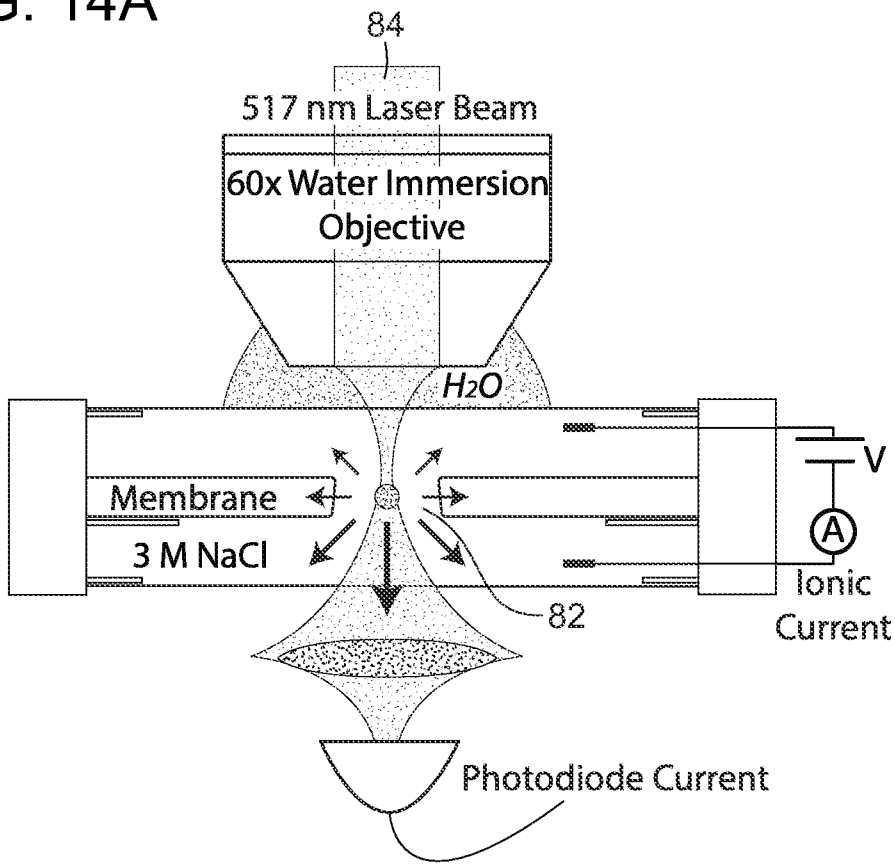


FIG. 14B

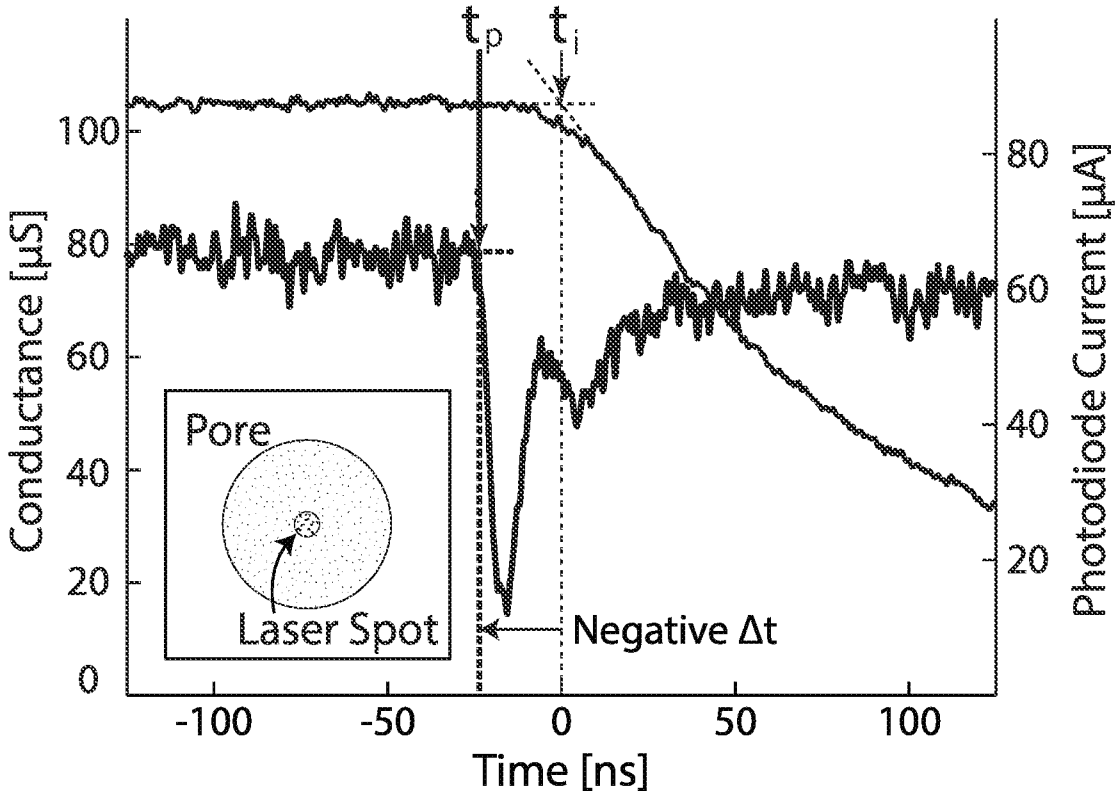


FIG. 14C

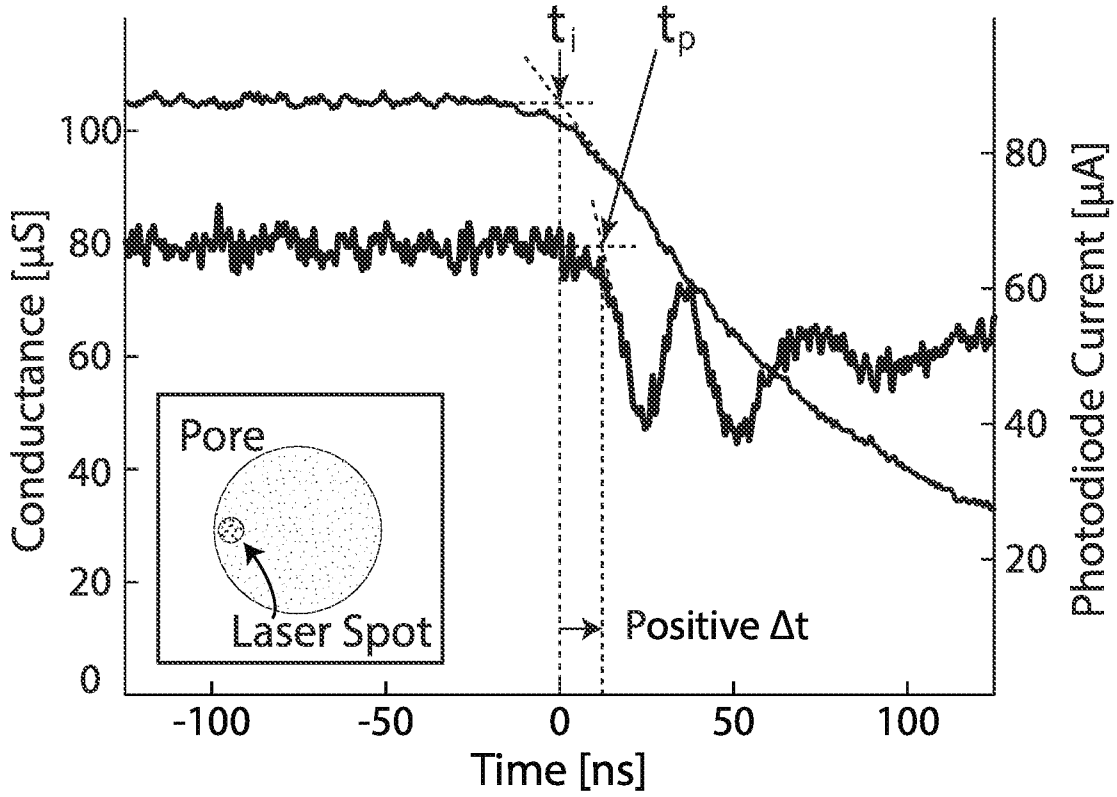
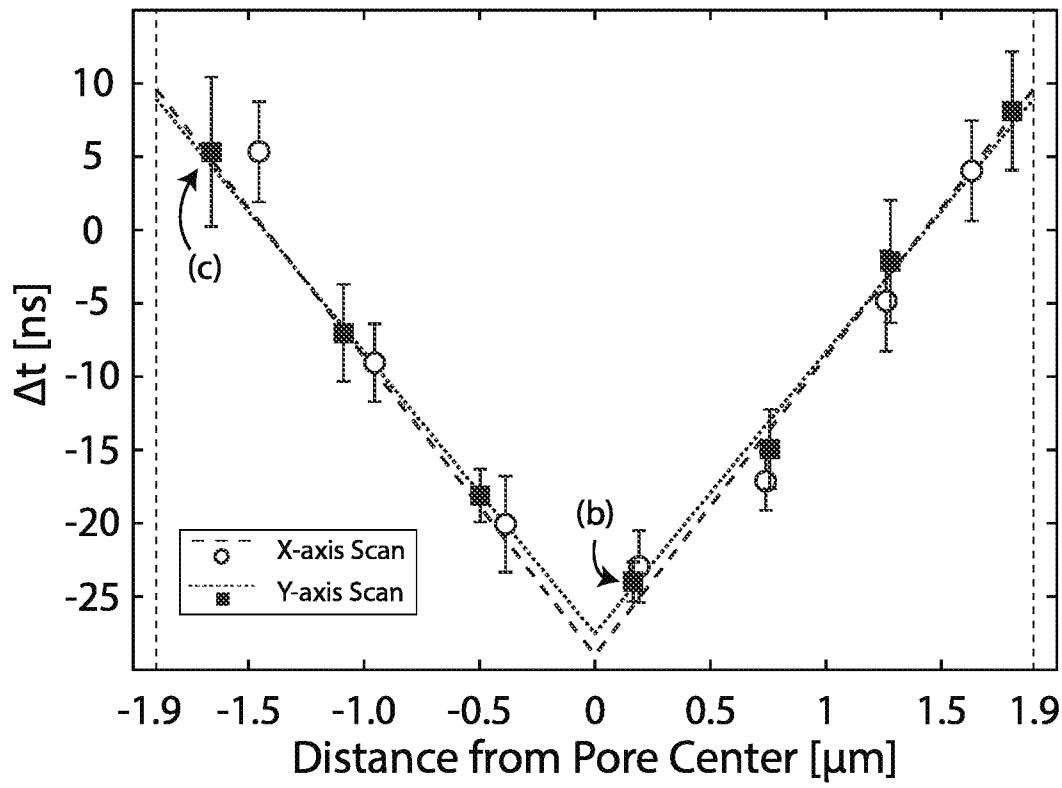


FIG. 14D



INTERNATIONAL SEARCH REPORT

International application No.
PCT/US15/37894

A. CLASSIFICATION OF SUBJECT MATTER
IPC(8) - C12Q 1/68; G01N 33/00 (2015.01)
CPC - C12Q 1/68; G01N 33/50, 33/48721
According to International Patent Classification (IPC) or to both national classification and IPC

B. FIELDS SEARCHED

Minimum documentation searched (classification system followed by classification symbols)
IPC(8) - C12Q 1/68; G01N 27/26, 27/416, 33/00 (2015.01)
CPC - C12Q 1/68, 1/6869; G01N 33/50, 33/48721 USPC - 204/453; 435/287.2; 436/94; 977/924

Documentation searched other than minimum documentation to the extent that such documents are included in the fields searched

Electronic data base consulted during the international search (name of data base and, where practicable, search terms used)
PatSeer (US, EP, WO, JP, DE, GB, CN, FR, KR, ES, AU, IN, CA, INPADOC Data); Google/Google Scholar; EBSCO, Proquest; pore, nanopore, aperture, capillary, object, polymer, DNA, RNA, molecule, detect, electrolytic, electrolyte, bubble, heat, superheat, golovchenko jene a, burns michael m, nagashima gaku, levine edlyn v, harvard college, bubble chamber

C. DOCUMENTS CONSIDERED TO BE RELEVANT

Category*	Citation of document, with indication, where appropriate, of the relevant passages	Relevant to claim No.
A	US 2012/0234679 A1 (GARAJ, S et al.) September 20, 2012; figure 1; paragraphs [0003], [0008]	1-20
A	US 2013/0244340 A1 (GENIA TECHNOLOGIES, INC.) September 19, 2013; abstract; figures 2A, 3; paragraph [0079]	1-20
A	US 2011/0159601 A1 (GOLOVCHENKO, JA et al.) June 30, 2011; paragraphs [0006], [0028], [0030], [0039]	1-20
A	CN 2014167413 (UNIVERSITY TSINGHUA) May 28, 2014; abstract; figures 1, 3; paragraph [0079]	1-20
A	US 2004/0166555 A1 (BRAFF, R et al.) August 26, 2004; figures 1 C-D; paragraphs [0058], [0174]	1-20
P, X	NAGASHIMA, G et al. Superheating and Homogeneous Single Bubble Nucleation in a Solid-State Nanopore. Physical review letters. 2014;113(2):024506; entire document	1-20

☐ Further documents are listed in the continuation of Box C. ☐ See patent family annex.

* Special categories of cited documents:
"A" document defining the general state of the art which is not considered to be of particular relevance
"E" earlier application or patent but published on or after the international filing date
"L" document which may throw doubts on priority claim(s) or which is cited to establish the publication date of another citation or other special reason (as specified)
"O" document referring to an oral disclosure, use, exhibition or other means
"P" document published prior to the international filing date but later than the priority date claimed
"T" later document published after the international filing date or priority date and not in conflict with the application but cited to understand the principle or theory underlying the invention
"X" document of particular relevance; the claimed invention cannot be considered novel or cannot be considered to involve an inventive step when the document is taken alone
"Y" document of particular relevance; the claimed invention cannot be considered to involve an inventive step when the document is combined with one or more other such documents, such combination being obvious to a person skilled in the art
"&" document member of the same patent family

Date of the actual completion of the international search	Date of mailing of the international search report
01 September 2015 (01.09.2015)	30 SEP 2015
Name and mailing address of the ISA/ Mail Stop PCT, Attn: ISA/US, Commissioner for Patents P.O. Box 1450, Alexandria, Virginia 22313-1450 Facsimile No. 571-273-8300	Authorized officer Shane Thomas PCT Helpdesk: 571-272-4300 PCT OSP: 571-272-7774

Form PCT/ISA/210 (second sheet) (January 2015)